A hypothetical approach toward laser-induced high-density polyethylene pyrolysis

Rao Adeel Un Nabi, Hassan Abbas Khawaja, Yao Xiang Liu, Chaopeng Yang, Juan Long, Xianwang Li, Tie Jun Wang

PII: S2214-9937(24)00254-9

DOI: https://doi.org/10.1016/j.susmat.2024.e01074

Reference: SUSMAT 1074

To appear in: *Sustainable Materials and Technologies*

Received date: 11 June 2024

Revised date: 20 July 2024

Accepted date: 1 August 2024

Please cite this article as: R.A.U. Nabi, H.A. Khawaja, Y.X. Liu, et al., A hypothetical approach toward laser-induced high-density polyethylene pyrolysis, *Sustainable Materials and Technologies* (2024), https://doi.org/10.1016/j.susmat.2024.e01074

A Hypothetical Approach Toward Laser-Induced High-Density Polyethylene Pyrolysis

Rao Adeel Un Nabi [a,b], Hassan Abbas Khawaja [c], Yao Xiang Liu [a], Chaopeng Yang [a,b], Juan Long [a,b], Xianwang Li [d], Tie Jun Wang*[a,b]

State Key Laboratory of High Field Laser Physics, Shanghai Institute of Optics and Fine Mechanics and CAS Center for Excellence in Ultra-intense Laser Science, Chinese Academy of Sciences, Shanghai, China

Center of Materials Science and Optoelectronics Engineering, University of Chinese Academy of Sciences, Beijing 100049, China.

Department of Automation and Process Engineering, UiT The Arctic University of Norway, 9019 Tromsø, Norway.

College of Physics, Guizhou University, Guiyang, Guizhou, 550025, China

*tiejunwang@siom.ac.cn

Abstract

Laser-induced breakdown spectroscopy (LIBS) is a commonly employed technique in commercial plastic recycling for purposes including classification, sorting, identification, and elemental analysis. However, understanding the molecular-level kinetics, thermodynamic interactions, bonding cleavage, and process parameter impacts is crucial for identifying necessary modifications to enhance plastic recycling. A review of the literature revealed that LIBS can also facilitate plastic pyrolysis, a significant research area that remains largely unexplored. Based on theoretical hypotheses, it can be concluded that laser-induced pyrolysis may offer advantages over traditional pyrolysis, which requires understanding the chemistry of plastic bond-breaking during degradation, identifying resistant bonds, and uncovering the root causes of these challenges. This approach is described in detail in sections 9 and 10, focusing on high-density polyethylene (HDPE) under controlled conditions. The identified research gaps could be further investigated, and advancements could be made toward establishing efficient plastic recycling and designing laser-induced pyrolysis reactors.

Keywords: HDPE, LIBS, Recycling, Bond Breaking, Pyrolysis

1. Introduction to plastic:

1.1. Effect of population growth

As populations grow, there is always a need for novel developments, and one of the most common examples worldwide is the use of items made from petroleum [1–3]. Plastic, a fundamental component of our daily existence, has become a worldwide concern. Human beings are responsible for their contribution to the negative consequences [4–6]. Unethical plastic disposal operations, such as burning, landfilling, and dumping, contribute to pollution in the atmosphere, soil contamination, and water quality issues, leading to severe diseases. Climate change is a persistent and pressing issue that has consequences for both the present condition of the earth and future generations, wrapping them in an unstoppable conflict against plastic pollution. Ensuring a plastic-free environment is crucial for the improved survival of future generations [7]. By eradicating plastic use and reducing carbon emissions, we must create an optimal setting for future generations, guided by ecological and ethical principles [8]. It is critical to investigate strategies that increase plastic's economic value through improved recycling procedures to achieve this goal [9]. Researchers have conducted most of their studies to address this issue, which can play a vital role in a sustainable environment and lead the way to achieving climate change goals [10]. Therefore, improving plastic recycling could help preserve ecological integrity, mitigate energy problems resulting from population expansion, and fulfil the need for petroleum products [11, 12].

1.2. Role of the Public in plastic recycling

Public awareness of the need for environmentally friendly production and consumption is growing [13, 14]. This has prompted local authorities to coordinate the collection of recyclables, motivated some manufacturers to produce items using recycled materials, and inspired other companies to meet the growing consumer demand [15, 16]. Consumer preference studies show that a notable, but not dominant, number of individuals prioritize environmental values when making purchase decisions. Customers who value the assurance of recovered materials and package recyclability could regard it as a favourable feature. However, if the recyclability is prospective and not actual, it might decrease consumer trust. Engaging in waste disposal initiatives is a common environmental practice, with a 57% participation rate in the UK in 2006 and an 80% rate in Australia [17-19]. Several nations, like the EU Directive on Manufacture and Materials for Packaging, adopt laws to promote the recycling of materials after consumer use [20]. Germany adopted laws that extended producer responsibility, resulting in the implementation of the Green Dot system for packaging recovery and recycling. The UK established manufacturer responsibility through a system that included the development and exchange of package recovery notes, and recently introduced a landfill charge to fund various waste reduction projects. The market value of recycled polymers and the viability of recycling have substantially increased in recent years [20-23].

1.3. Role of LIBS in Plastic Recycling

This section provides a summary of the most recent advancements in LIBS technology for polymer analysis, with a focus on its ability to break polymer bonds and produce novel materials, such as petroleum products produced by laser-induced pyrolysis. There hasn't been much focus on this specific aspect of the research. By utilizing discarded plastic in this way, value-added products can be generated that will contribute to a sustainable future. LIBS is a widely used atomic emission spectroscopic method that offers qualitative and quantitative insights into elemental analysis. The LIBS approach is characterized by its ability to detect numerous elements in a single-shot collection and its minimum sample preparation requirements. Its capacities to rapidly analyze and its non-destructive nature with minimal sample requirement, along with its standoff capability, have made it a very promising application in diverse domains such as element identification and mapping, composition monitoring, classification and differentiation, and the efficient exploration and use of natural mineral resources [24-26]. This technique has been extensively employed with diverse multivariate approaches for material identification across many applications. Several studies on plastic utilizing LIBS have been conducted in recent decades, covering toys, food containers, e-waste, and a wide range of other plastic goods [27-29]. The fundamentals of plastic, equipment selection, and comparisons of different chemometric methods have been addressed. Most earlier studies concentrated on plastic identification, with a handful on the composition of elements. Identifying plastic kinds and quantifying specific constituents are crucial for efficient plastic recycling. LIBS could be used to assess the number of exciting materials after determining the type of plastic, considering the needs of real-life circumstances [30-32].

Although there have been advancements, there are still considerable gaps in research when it comes to taking insight into the bond-breaking behaviour of HDPE during the LIBS operation [33–35]. Most investigations have primarily focused on the phases of identification and classification, with less attention being paid to the processes of molecular interactions and disintegration. This gap underlines the need for more research into how LIBS may be utilized not just for sorting but also for modifying the chemical structure of HDPE in an approach that promotes recycling. For example, knowing how laser may aid in bond-breaking and pyrolysis of HDPE might open up novel possibilities for efficient plastic recycling, changing it into valuable chemicals or fuels, hence expanding its economic recycling potential. Bridging the research gap, especially in understanding the molecular-level impacts of LIBS on HDPE, has the potential to significantly improve recycling operation's efficiency and sustainability, making them more economically feasible and ecologically beneficial. Shortly after, LIBS became prominent for identification and sorting in recycling plastics like HDPE. At the same time, pyrolysis is considered more efficient for obtaining petroleum products from plastic or synthetic organic waste. Nevertheless, a significant gap exists in achieving satisfactory recovery from plastic waste. Addressing this gap requires conducting laser-induced pyrolysis, which can help uncover the fundamental causes of this deficiency. Currently, there is no evidence to support the hypothesis that laser-induced pyrolysis has been explored, either experimentally or theoretically, as no researcher has conducted such a study. We are actively working towards this objective and anticipate presenting additional convincing evidence to support our claim in the future. Below are this study's primary and secondary objectives, which aim to clarify the goal further.

Primary Objective:

- Evaluating LIBS for plastic polymers, emphasizing HDPE

Secondary Objectives:

- To investigate LIBS for HDPE bond-breaking
- To analyze undocumented LIBS Spectra of Key Products
- Analysis of C-C and C-H bonds durability in HDPE
- To investigate the potential of Laser-Induced HDPE Pyrolysis

2. Literature Survey and Methodological Framework

In this section, the referenced literature demonstrates the widespread application of LIBS in various studies aimed at identifying distinct material categories. These studies provide insight into the favourable aspects of LIBS, providing evidence for its effectiveness as a diverse analytical tool. After conducting extensive analysis using various sources, such as PubMed and Google Scholar, insufficient information has been found regarding laser-induced pyrolysis. However, sources and published literature have discussed the molecular-level interaction between lasers and HDPE [36-41], as well as the potential for laser-induced pyrolysis [1,3,9]. This knowledge has led to the development of a hypothetical methodological overview, detailed in sections 9 and 10 of this manuscript, requiring further extensive experimental and theoretical examination. The first question that comes to mind is the potential lack of effectiveness of laser-induced HDPE pyrolysis for the industry. In this particular scenario, how will this study proceed? Currently, the viability of laser-induced HDPE pyrolysis for commercial applications remains unclear, making a thorough analysis of this subject unfeasible. Only experimental and theoretical data can be used to finalize this subject. However, conducting an investigation on this specific path will provide valuable insights that could potentially boost the commercial feasibility of this technique. This study aims to examine the fundamental principles of physics and chemistry that are involved in the process of laser-induced HDPE pyrolysis. The objective is to gain a better understanding of this process in order to effectively tackle the issues associated with plastic recycling. This study provides a significant edge over the natural environment. In addition to its design, this approach ensures a complete end of operations, thereby preventing any environmental harm. The experiment's conduct in a vacuum environment, capable of reducing harmful gas emissions, enhances its safety and environmental friendliness. This experimental setup provides an advantage to the substance being studied by allowing for more precise control and minimising any environmental obstacles. Overall, the endeavour demonstrates a strong dedication to the environment.

According to the survey, Singh *et al.* [36] used LIBS to analyze nutrient elements in the seed kernels of cucurbits, identifying magnesium, calcium, sodium, and potassium using principle component analysis (PCA)for data categorization. Junjuri *et al.* [37] identified ten distinct plastic types using LIBS, reaching 93% classification accuracy using correlation and ratio metric analysis, with the possibility of additional development using machine learning. Castro *et al.*[38] employed LIBS to detect plastic polymers in electronic trash, combining chemometric methods with data mining approaches to alter acquired data for polymer identification. Malenfant *et al.*[39] employed LIBS to distinguish bacterial cells from pollutants based on size, resulting in a straightforward laboratory process for microbiologists. Wang *et al.* [40] emphasized the relevance of chemometric models linked with LIBS for recognizing various plastic materials through a k-nearest neighbour, artificial neural networks (ANN), and linear discriminant analysis (LDA). Król*et al.*[41] used micro-fluorescence X-rays and LIBS to detect distinctive atomic emissions from components in Polish banknotes. Tang *et al.* [42] used unsupervised learning methods such as K-means and self-organizing maps (SOM) to identify commercial polymers using LIBS with ideal classification accuracy. Chen *et al.* [43] demonstrated the detection of heavy metals in microplastics using LIBS, removing the requirement for bulk samples and improving identification effectiveness using a thin polyethene substrate. Brunnbauer *et al.*[44] used PCA and k-means clustering to identify synthetic polymers using LIBS, which enables direct analysis of two-dimensional structured polymers. The implementation of LIBS in a wide range of sectors, including agriculture, waste management, medical diagnostics, and material science, according to Singh *et al.* [36], Junjuri *et al.* [37], Costa *et al.* [38], and others demonstrates the adaptability and potential of this analytical technology. However, the breadth of applicability raises concerns about limitations and unexplored possibilities within every field. For example, whereas Singh *et al.* [36] dealt with nutrient components in cucurbit seed kernels, one could ask whether this technique might be applied to other plant species or various portions of the plant for a more thorough nutritional study. Similarly, the successful outcomes of Junjuri *et al.* [37] and Castro *et al.* [38] in classifying plastic types and recognizing plastics in electronic waste using LIBS and advanced data analysis techniques offer the question of whether or not these methodologies could be refined or expanded to address the more significant issue of microplastic pollution in environmental matrices. Brunnbauer *et al.* [44] and Król *et al.* [41] have demonstrated the use of LIBS for quality assurance when examining synthetic polymers and identifying components used in producing banknotes. A single material has been targeted and analyzed using LIBS in these cases.

3. Principle of LIBS in Plastic Analysis

Traditional LIBS and ultrafast LIBS are modern analytical techniques that precisely identify and characterize plastics such as HDPE. The fundamental principle of these spectroscopies is to focus on the sample surface with an intense laser pulse to generate plasma. In the case of ultrafast LIBS, this plasma generation occurs within the filament created in filamentation, which may occur only within a transparent medium [45-47]. Both techniques are capable of generating plasma; however, traditional LIBS does not involve the phenomenon of filamentation, unlike ultrafast LIBS. This difference is due to the larger wavelengths and longer pulse durations associated with traditional LIBS compared to ultrafast LIBS, which can alter the nature of plasma [48, 49]. This plasma is a high-temperature ionized gas cloud composed of electrons, ions, and neutral atoms stimulated to higher energy levels by the laser pulse. Once the plasma cools down and expands, the charged particles inside it produce light with specified wavelengths referred to as emission lines, which are usually distinctive of the elements in the sample and are measured using a spectrometer [50-52]. Figure 1 shows the details mentioned above.

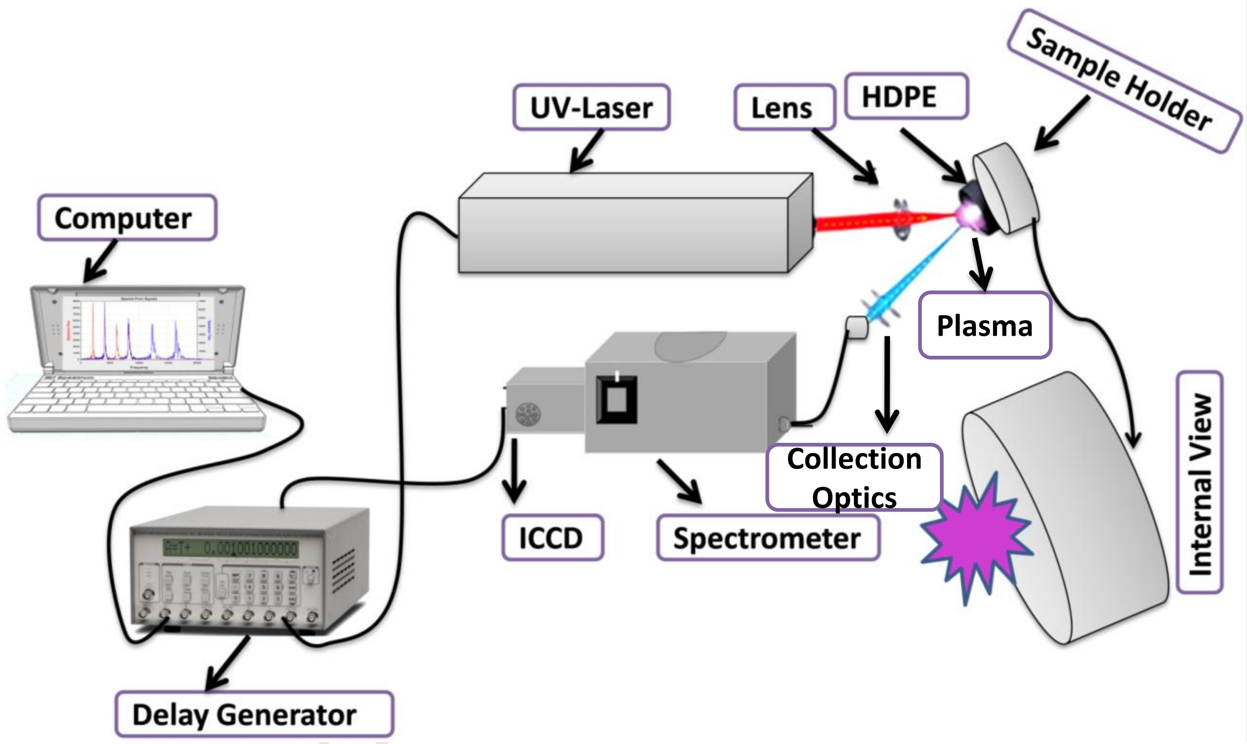

Figure 1: The graphical view of the LIBS principle

The concentration of components in samples evaluated by LIBS is proportional to the strength of spectral lines emitted, yielding accurate compositional data [53]. The LIBS technique analyzes the laser-induced plasma emissions of plastics to identify their elemental composition, which is crucial for understanding their physical properties and potential uses, as well as the qualitative and quantitative information that can be obtained. This approach efficiently detects materials by identifying significant and insignificant constituents, improving their durability, robustness, and functionality. Furthermore, it is essential to differentiate physically similar but chemically distinct polymers like HDPE and LDPE since their composition cannot be determined based on their appearance alone.

4. Recent approaches in plastic analysis:

4.1. Spectroscopic Approaches

Figure 2 depicts various spectroscopic approaches' roles in plastic analysis. The primary challenges associated with manual identification and classification are the significant time investment and subsequent lack of cost-effectiveness due to the labour-intensive nature of the process. In addition, hand sorting relies on eye inspection and is thus susceptible to mistakes and impractical on a large scale. Several other techniques that use the physical features of that material have been employed for plastic identification, such as the density separation approach and classification through electric properties [54-58]. Most of these approaches are limited to certain plastics due to their reliance on physical qualities, which are more susceptible to the effect of many factors, mainly when dealing with plastic debris collected from exterior settings.

Furthermore, the primary impediment that hinders the effectiveness of conventional methods in plastic separating is the lengthy analysis time required to examine samples. This time-consuming process often fails to meet industrial standards, mainly when there is a need for rapid operations to process a large number of samples within a limited timeframe. The usual procedures are thus not highly appropriate, particularly for the second and third phases of applications. Classification can be much more precise when using methods that depend on the basic features of material at molecular levels. Spectroscopic approaches are thus appropriate for effective categorization and arrangement in such applications [59-62].

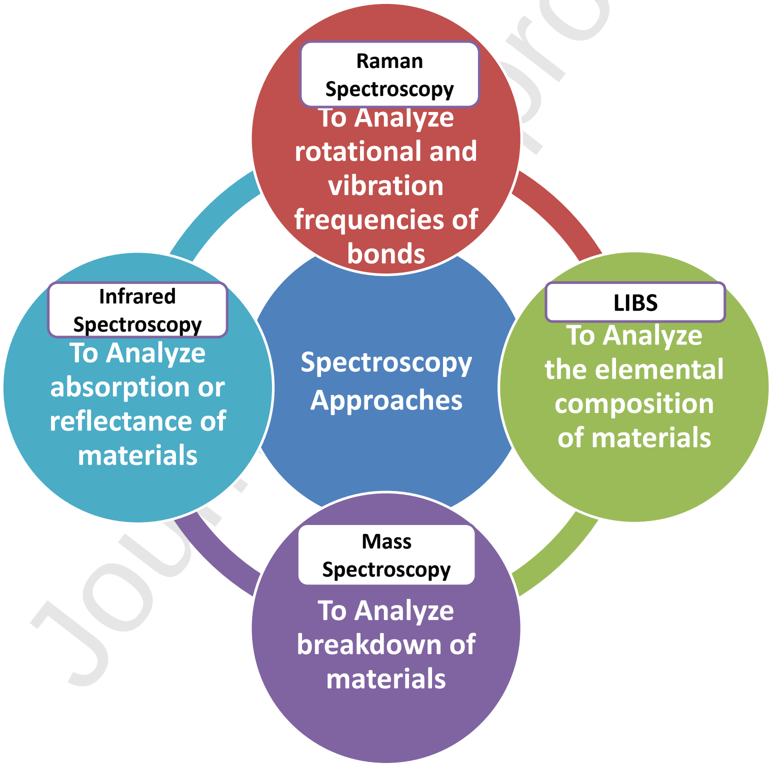

Figure 2. The roles of spectroscopic approaches in the analysis of plastics

4.2.Chemometric Approaches

Chemometric tools are often used to examine the chemical data collected by spectroscopic procedures. Chemometrics is crucial to the long-term control of petroleum-based products, contributing to environmental sustainability and the circular economy. Few supervised models, such as Support Vector Machines (SVM), Artificial Neural Networks (ANN), Partial Least Squares Regression (PLSR), and unsupervised models, such as Principal Component Analysis (PCA), k-means neighbour (KMN), Self-Organizing Maps (SOM) have been reported to analyze plastic for commercial-scale applications [63]. The graphical representations of the models are listed below in Figure 3. For example, PCA is a dimensionality reduction technique used with multidimensional datasets. This statistical technique creates additional axes called principle components, linear mixtures of the original variables. Each primary component is designed to maximize variance, so collecting the maximum information. The variation ratio can show how each primary component contributes to the total data variance. The data can be visually represented in two dimensions by showing the main components with the best-explained variance ratio. Data from the identical category would generally be grouped adjacent to the plot and distinguishable from other clusters. PCA can be used to lower the size of plastic spectra before sending the main components as input data to several classifier models. This approach offers simple classification since each sample can be categorized into several groups based on the classification threshold distance [64].

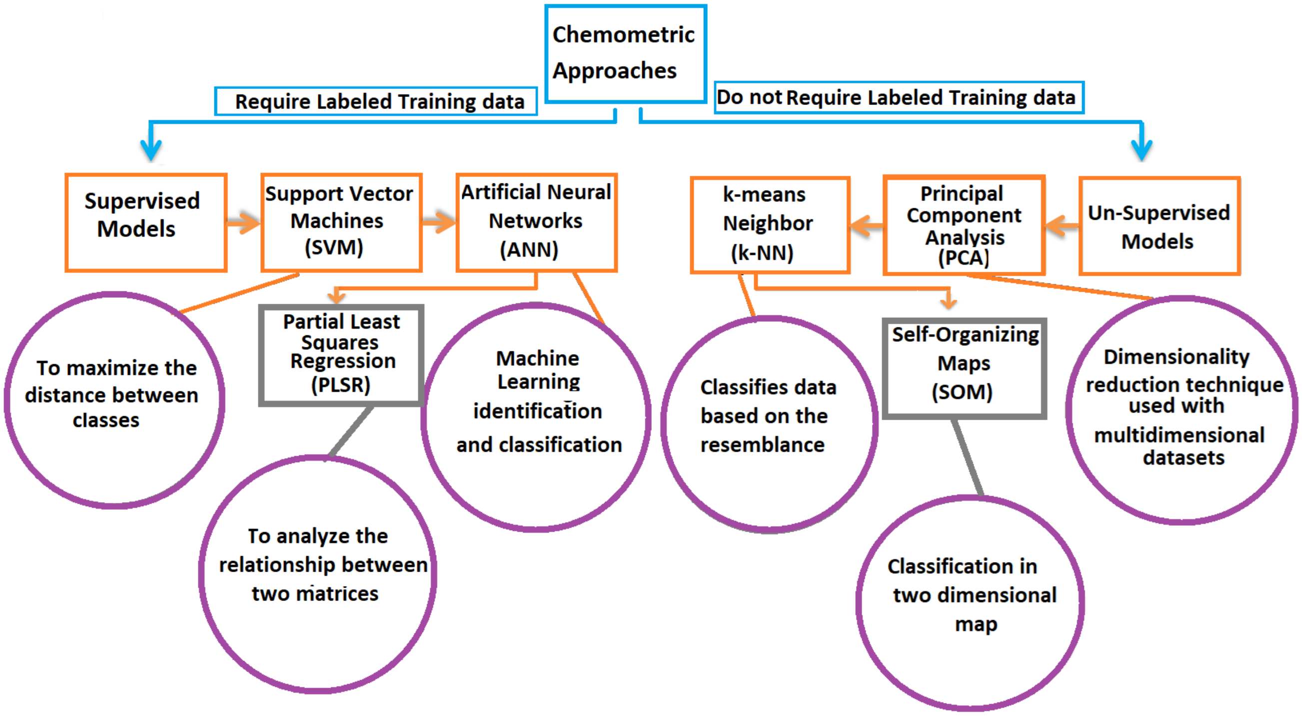

Figure 3. Overview of the supervised and un-supervised models

LDA is similar to PCA; however, with LDA, additional axes can be designed to maximize class separation. This is accomplished by increasing the distance among the means of every class while reducing the dispersion of the dataset inside each class [32]. The data can then be moved to the newly defined lower dimension axis. LDA could be used to classify different polymers and flame retardants based on bromine [65].

PLS is a form of statistical analysis that uses latent variables to analyze the relationship between two matrices. The latent variables (LV) can possibly be used to determine the vector located in the X-domain corresponding to the vector in the neighbouring Y-domain with the most variance.

When employed for classification purposes, a version known as PLS-DA can be used, in which the Y-matrix represents a dummy matrix with values 1 and 0. PLS-DA is a popular chemometric technique for categorizing different types of plastics [66, 67]. K-NN is a classification strategy that classifies data based on the resemblance of the K-NN to the new understanding, with k being a variable parameter. The latest observation class will be determined by the majority class of its closest neighbours. K-NN can also be used with PCA for large-dimensional datasets [38, 56].SVM is an approach to classification that uses decision boundaries to maximize the distance between classes. In a non-probabilistic approach, new samples can be categorized according to which side of the boundary of the decision they land on. SVM has traditionally been a binary classification technique, but recent advancements enable it to address multi-class classification issues, including plastic classification [69].

Random forecast (RF) is an ensemble machine-learning (ML) approach that employs many decision trees. The random forest technique produces the average prediction outcomes of all decision trees. Bagging is used throughout the learning process when each decision tree is constructed from separate training data. This helps to avoid overfitting the dataset. RF regression can be employed with LIBS to determine the presence of harmful heavy metal ions in polymers [70].

5. Selection of Specific Models for Analysis

Supervised models are ideal for classification and regression tasks that require labelled training data, such as spectra with known classes or concentrations that can provide specific information about the composition or type of plastics. It is more suitable for recognizing different types of plastics or predicting the amounts of particular elements in plastics. Unsupervised models enable the finding previously unknown links in plastic materials and cluster analysis of related spectra without prior knowledge [71].

The objective of the analysis determines it. Supervised models are often used to identify specific features of plastics, especially plastic-type and elemental amounts of chemicals. Unsupervised models help investigate data structure without a particular goal. Supervised models require labelled training data(LTD), which is frequently unavailable. Unsupervised models may give helpful information if the dataset lacks labelled samples. If the plastic analysis problem is complicated and contains intricate interactions, supervised models that learn from labelled instances may perform better. Unsupervised models, on the other hand, may be helpful for smaller tasks or exploratory analysis [72]. However, combining both approaches could be a good choice since unsupervised approaches can be used for early exploration and extraction of features, followed by supervised models for particular prediction and classification tasks. The decision is ultimately determined by the type of study, the accessible data, and the anticipated conclusions, as shown in Figure 4.

The following section will deeply explore the elements and molecules relevant to domestic and industrial plastics under opened and closed environments, often called synthetic organic polymers or organic compounds. Based on this spectral information, a spectrometer can identify the bond-breaking phenomenon in HDPE during the experiment.

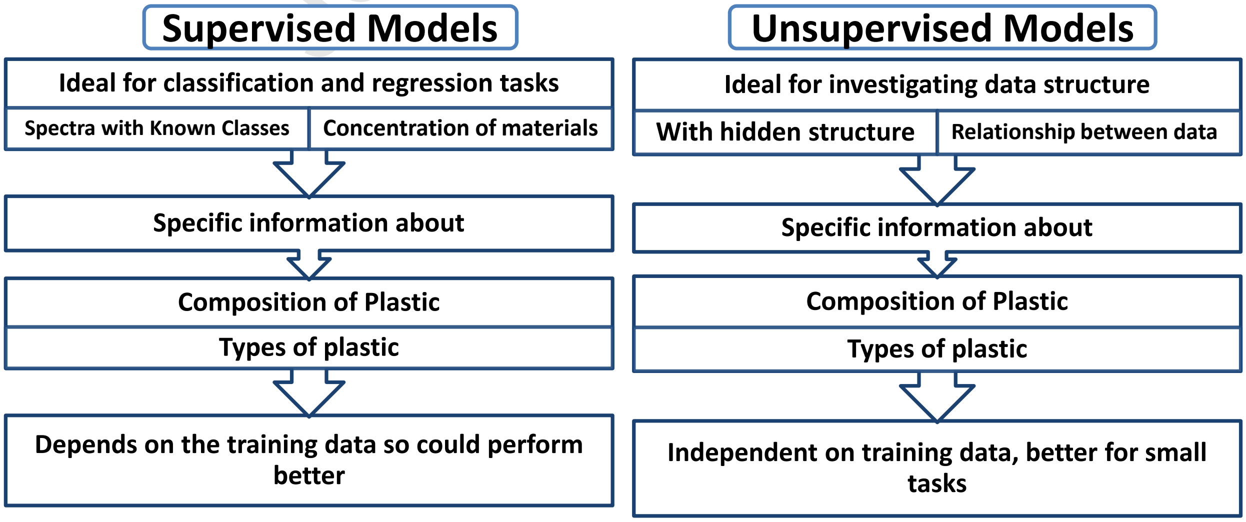

Figure 4. An overview of the selection of the model

6. LIBS elemental spectrum of synthetic organic polymers

This section provides a comprehensive discussion on plastic's breakdown spectrum after the laser's interaction with plastics. It also highlights the precise wavelengths associated with atoms, ions, and molecules that have been found, as reported below in Table 1. Usually, LIBS spectra obtained from plastic materials have specific emission lines that are specific to the elements present in the plastic, such as carbon (C), hydrogen (H), nitrogen (N), and oxygen (O) [73]. In addition, certain molecular emission bands associated with carbon diatomic (C_2), carbon-nitrogen (CN), carbon-hydrogen (CH), nitrogen-hydrogen (NH), and oxygen-hydrogen (OH) fragments have also been observed [74]. These fragments can originate from the parent molecule or be formed through chemical reactions involving the immediate species in the plasma or the reactive surrounding atmosphere. The formation of such emissions is based on several factors that influence the ablation process.

Additionally, there may be additional species present in the emitted plume that do not exhibit observable spectrum signatures. However, their existence can be verified using supplementary methods [70]. There are several reasons why these features may not be detected, for example, not enough energy transferred to activate the species, a minimal amount of the molecules, emission wavelengths that are not within the range of effective spectral measurement, or emission lifetime that is not within the range of effective temporal measurement such as during the degradation of HDPE, a few hydrocarbons [75-77] are generated like ethylene (C_2H_4) [78], and butylene (C_4H_8) whose spectrum is less than 200 nm which is not detectable using a standard spectrometer. Regardless, any species, even those not discovered, may participate in competitive reaction pathways to generate new species.

6.1.Carbon (C)

The C emits its most intense spectral lines in the absence of oxygen, specifically at wavelengths 156.1 nm, 165.7 nm, and 193.2 nm [79]. However, a challenge arises when trying to directly determine the presence of carbon using these emission features, as many commercially available LIBS spectrometers do not operate within this wavelength range. The emission line at 247.86 nm is often chosen as the primary focus in LIBS experiments. At times, a trace of emission of approximately 493 nm can be detected [80]. However, it is often identified as an additional order of 247 nm instead of being assigned to the emission wavelength. It is important to note that the durations of atoms' excited states are very brief compared to those of molecules. Hence, gathering emissions from carbon and other atoms during the initial phases of plasma generation is essential. In organic polymer, the later phase could limit the observation of the spectrum due to the dominance of complex reactions and plasma cooling processes [81]. The decreased magnitude of atomic radiation during the later phases of plasma expansion, exceeding 5 ms, combined with the involvement of unbound carbon atoms in chemical reactions that result in the creation of newly formed diatomic molecules such as CN, CH, CO, and C_2, as well as larger carbon clusters, can have noteworthy consequences for its detection.

6.2.Hydrogen (H)

The H atoms in plasmas generated by lasers emit a sequence of spectral lines inside the visible range, namely the Balmer series. The Balmer series is composed of five distinct spectral lines such as H(α) at 656.28 nm, H(β) at 486.13 nm, H(γ) at 434.05 nm, H(Δ) at 410.17 nm, and H(z) at 388.91 nm. The H(α) and H(β) lines of the Balmer series are often seen in the LIBS spectra of plastic plasmas [82]. The H(α) line is more intense, while the H(β) line is broader as a result of Stark broadening, which means the regional electric field in the plasma causes disturbances to the emitters, which could be atoms or ions, resulting in the occurrence of a dynamic Stark effect (SE). In addition to their reduced strength, it is essential to acknowledge that the H(β) and H(z) lines can be obscured by potential C_2 and CN emissions, leading to their lack of detection. The literature provides a wide range of observations, examinations, and evaluations of emissions from atomic hydrogen lines after analyzing LIBS spectra of different kinds of samples [83]. Analysis of H with traditional LIBS is often performed at atmospheric air pressure, so H, included in water molecules (H_2O) found everywhere in the air, can interfere with the analysis of hydrogen atoms that originate from an organic element. This makes it difficult to distinguish between the H atoms emanating from the substance being analyzed and those from the surrounding air. Working in environments without water and oxygen and employing isotopes with deuterium has aided in understanding the processes involved in forming molecules since it leads toward accuracy by minimizing the additional interface with products [84].

6.3.Nitrogen

Plasma with a high level of ionization can lead to the splitting of gas molecules in the surrounding environment, such as air molecules, resulting in the formation of N atoms and combining them with the N atoms already present in the plastic material. Indeed, the N atoms derived from the environment play a significant role in enhancing the intensity of the ultimate emission. This is because the quantity of matter dissolved off the target surface is often lower than the amount of the ionized environment due to the dimensions of the plasma. The most substantial apparent emissions of neutral N occur at 575.25 nm, 742.36 nm, 744.2 nm, 746.83 nm, 821.63 nm, and 860 nm **[**85**].** Furthermore, it is possible to detect emissions from nitrogen atoms that have been singularly and double ionized under certain conditions. The most intense emissions of ionized nitrogen can be observed at 399.50 nm, 444.70 nm, 463.05 nm, 500.51 nm, 567.96 nm, 648.20 nm, and 661.06 nm **[79**]. Similarly, the participation of N atoms in the plasma modifies their initial involvement in the light-emitting spectrum, much as C and H atoms. This alteration complicates tracing the pathways by which diatomic species such as CN and NH are formed [86].

6.4.Oxygen

The plastic samples exhibit intense O emission at specific wavelengths, notably 777.19 nm, 777.41 nm, 777.53 nm, 794.7 nm, and 844.6 nm **[**87]. The relaxation of excited atomic states primarily causes this emission. Although the emissions from this element are the most prominent, there are additional ionic O^+ lines that are about eight times less intense and weak $O2^+$ lines that are around 150 times less intense. However, these weaker emissions can only exist under certain conditions [88]. The plumes exhibit greater reactivity with O_2 owing to the lower bond breakdown energy of O_2 compared to N_2. Several species originate from molecular oxygen, while others easily interact with it and the highly reactive oxygen atoms. Under certain working circumstances, it is possible to detect spectral signals from unbound diatomic radicals (DR), such as OH, CO, and NO.

Nevertheless, it is often challenging to monitor the optical emissions of various oxygen species, such as hydrogen peroxide (H_2O_2), nitric oxide or nitrogen monoxide (NO), peroxides, and superoxides. However, whether these species are visible or not, they still affect the absorption and emission operations of the plasma plume via oxidative chemical reactions. All the elemental and molecular spectral wavelength rages are reported in Tables 1 and 2 accordingly [89, 90]. Figure 2 represents the graphical view of peak variation corresponding to the wavelengths.

Table 1. All the LIBS elemental spectral wavelength ranges of synthetic organic polymers

Elements	Wavelengths (nm)	Ref.	Elements		Wavelengths (nm)	Ref.
Carbon	165.7	[79, 80]	Hydrogen	H(α)	656.28	[82]
	193.2			H(β)	486.13	
	247			H(γ)	434.05	
	247.86	[91, 80]		H(Δ)	410.17	
	493			H(z)	388.91	
Neutral Nitrogen	575.25	[85]	Ionized Nitrogen		399.50	[93]
	742.36				444.70	
	744.2				463.05	
	746.83				500.51	
	821.63				567.96	
	860				648.20	
Oxygen	777.19	[87]			661.06	
	777.41				399.50	
	777.53					
	794.7	[92]				
	844.6					

7. LIBS Molecular Spectrum of Plastic or synthetic organic polymer

7.1.Diatomic Carbon (C_2)

One of the most extensively studied carbon group ions is the C_2 radical [94]. The formation of very stable carbon groups can happen through the vaporization of plastic surfaces using intense laser pulses. The distribution of C clusters is influenced by several variables, including the specific C-bonding types inside the molecule, the conditions of irradiation, the location of the plasma volume being sampled, the time of investigation, and the characteristics and level of pressure in the surrounding environment. This suggests that the emergence of these species can be attributed to the direct splitting of the plastic material. The C_2 radical is related to many band systems, including the Swan bands, often referred to as the initial positive bands of C. The frequency of their occurrence is based on certain variables. For instance, several spectra of recently developed highly energetic substances have shown a prominent emission characteristic in the range of 543 nm, which may be attributed to the high-pressure region's band of C_2, as shown in Figure 5. The Swan spectrum is responsible for identifying the most often seen C_2 bands in LIBS signals originating from carbon-containing sources [95]. The Swan bands of C_2 consist of five vibrational phases with bands at 438.2 nm, 473.7 nm, 516.5 nm, 563.5 nm, and 619.1 nm [96]. At these regions, the system may achieve both vibrational and rotational resolution. However, it is essential to note that the vaporization and plasma expansion conditions can result in these sequences' absence or complete absence in the LIBS spectra, even for C-containing molecules. This fact is a fundamental component in LIBS investigations of C_2 species [97].

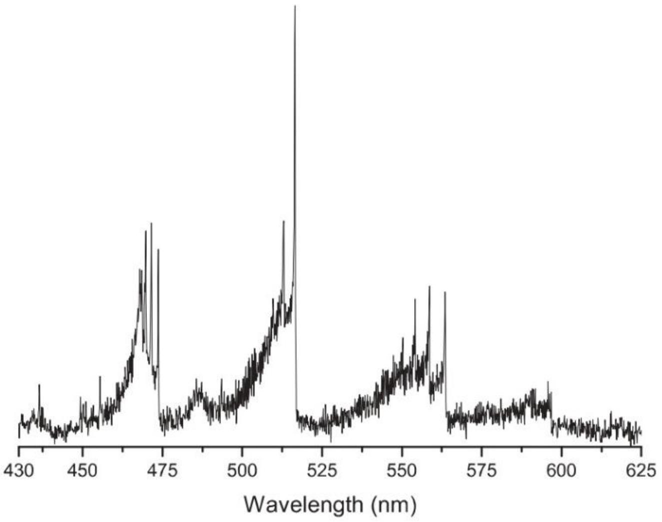

Figure 5. The molecular emission spectrum of C_2 [96, 79]

7.2.Carbon-Nitrogen

The formation of this radical may occur either by direct CN bonding inside the parent molecule or through gas-phase interactions involving C and N atoms [98]. The red and violet fluorescence band systems allow for observing CN radicals and electronic transition of vibrational quantum number (Δv), as shown in Figure 6. The violet system includes the (Δv=0) sequence with band heads at 388.3 nm (0–0), 387.1 nm (1–1), 386.2 nm (2–2), 385.5 nm (3–3), 385.1 nm (4–4), the (Δv=-1) vibrational sequence along with band heads at 419.7 nm (1–2), 418.1 nm (2–3), 416.8 nm (3–4), 415.6 nm (4–5), 415.2 nm (5–6),421.6 nm (0–1), and the (Δv=+1) sequence at 358.6 nm (2–1), and 358.4 nm (3-2), 359.0 nm (1–0). The CN violet system is the subject of extensive research due to its prevalence in many emission sources [99]. The violet system bands have been extensively employed in numerous investigations to diagnose plasma parameters, the potential impact of the molecular structure of plastic materials on the observed emissions from CN species, and analyze the influence of excitation parameters on their development, temporal, and spatial dynamics. Additionally, these investigations have explored these emissions' sensitivity to the background gas's composition and pressure [100]. Furthermore, the recent examination of spectroscopically resolved isotope changes in the wavelengths of the primary bands within the CN red system has facilitated the resolution of several unresolved uncertainties related to this subject [79]. Nevertheless, the emission of C_2 at 438.4 nm, which is typically more intense, hides the head of the R(0,0) branch. Likewise, the CH band at 431.4 nm could be partly overshadowed in a prominent Hg line, resulting in a less pronounced CH system. Notably, the head located at a wavelength of 432.3 nm exhibits the highest degree of variability, with its intensity typically varying in accordance with the magnitude of the optimum vibrational temperature. The remaining CH band groups at 390 nm and 315 nm show a decline towards the red wavelength. The former exhibits prominent peaks at 387.1 nm and 388.9 nm, indicating a substantial degree of emission for the (Δv=0) phase of the CN violet system, which may hinder its detection. The 314 nm band system has a much lower intensity than the other two systems, with only a limited number of weak densely clustered peaks at 314.4 nm and 315.7nm **[**101**,** 102]. The aforementioned system is subject to interference and may be hidden by emissions from other species, such as incredibly excited nitrogen and nitrogen dioxide (NO_2) [103].

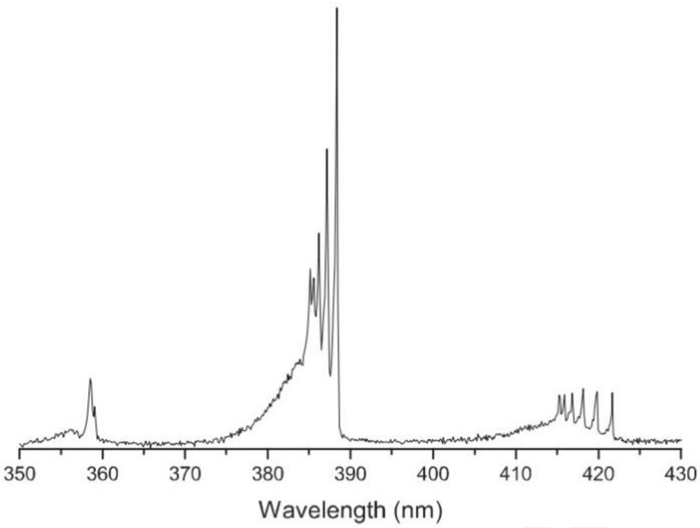

Figure 6. The molecular emission spectrum of CN [96, 79]

7.3.Carbon-hydrogen (CH)

Carbon-hydrogen is the most extensively studied free radical due to its high susceptibility to excitation during hydrocarbon burning and electrical emissions, including carbon and hydrogen. In the visible and near UV ranges, the CH radical emits light in three distinct band systems such as 410–440 nm, 360–420 nm, and 315 nm [100]. The 430 nm band system has the highest brightness and gradually moves towards the violet region. The movement of molecules within electronic and rotational bands is generally referred to using the P, Q, and R branches, representing state changes. For example, a comprehensive structure at a wavelength of 431.5 nm, consisting of Q(0,0) and Q(1,1), is seen in the most sensitive portions of this system, according to Figure 7. This structure invariably follows a thinner and distinct signal at 432.3 nm, Q(2,2). The presence of double branches (Q and R) in a molecule signifies an odd number of electrons, a noteworthy characteristic of an excited species.

Moreover, it can be seen that branches possess an open rotational framework, which is a distinctive feature of a diatomic hydride. Nevertheless, the emission of C_2 at 438.4 nm, which is typically more intense, hides the head of the R(0,0) branch. Likewise, the CH band at 431.4 nm might be partly overshadowed in a prominent Hg line, resulting in a less pronounced CH system. Notably, the head located at a wavelength of 432.3 nm exhibits the highest degree of variability, with its intensity typically varying in accordance with the magnitude of the optimum vibrational temperature. The remaining CH band groups at 390 nm and 315 nm show a decline towards the red wavelength [104]. The existence of the CN violet group may be masked by the substantial emission intensity, as demonstrated by the strong heads found at 387.1 nm and 388.9 nm. The 314 nm band system has much lower intensity than the other two systems, with only a limited number of weak, densely clustered peaks at 314.4 nm and 315.7 nm. The system mentioned above is susceptible to interferences and may be hidden by emissions from other species, such as incredibly excited nitrogen and nitrogen dioxide.

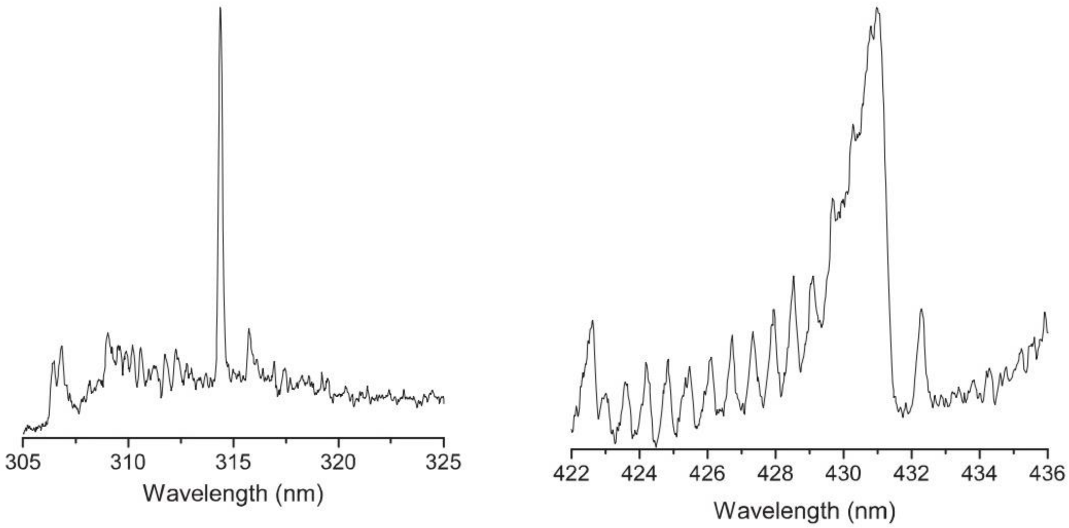

Figure 7. The molecular emission spectrum of CH [96, 79]

7.4.Oxygen-Hydrogen

The wavelengths of emission of OH radicals are often detected in various plasmas, particularly in plasmas with significant water content and OH-containing compounds like sugars and alcohols. Nevertheless, while such conditions may produce massive amounts of OH, its high degree of reactivity and limited chemical lifetime often result in low measured quantities [105]. These challenges obtain high signal-to-noise (S/N) ratios for OH emissions with a single spectrum capture, requiring light collection from consecutive plasma events. In addition, the collecting process must occur with significant delay durations ranging from 30 to 300 milliseconds from the LIBS. The band structure corresponding with the UV irradiation in the 300–330 nm wavelength range is characterized by the most significant molecular fluorescence from OH radicals. Figure 2 illustrates a rovibrational structure of the band system, consisting of six primary branches such as 306.4 nm (R_{11}), 306.8 nm (R_{22}), 307.8 nm (Q_{11}), 309.0 nm (Q_{22}), 308.2 nm (P_{11}), and 309.6 nm (P_{22}) [96]. According to Figure 8, at first sight, the (0,0) band system at 306.4 nm seems noisy and has a low spectral resolution. However, it is very repeatable and exhibits all the required lines with a medium level of resolution.

It is important to note that, in addition to the primary emission in the ultraviolet range, additional band systems are associated with OH. One spectrum is in the ultraviolet (UV) range of 224.8–260.0 nm, while another is in the visible range of 420–600 nm. The third spectrum, known as the OH Meinel band spectrum (MBS), has a broadband characterized by distinct P, Q, and R branches, operating from 550–900 nm. Unfortunately, according to cited literature, identifying these bands in LIBS-generated plasmas of synthetic organic polymers has not been accomplished [106].

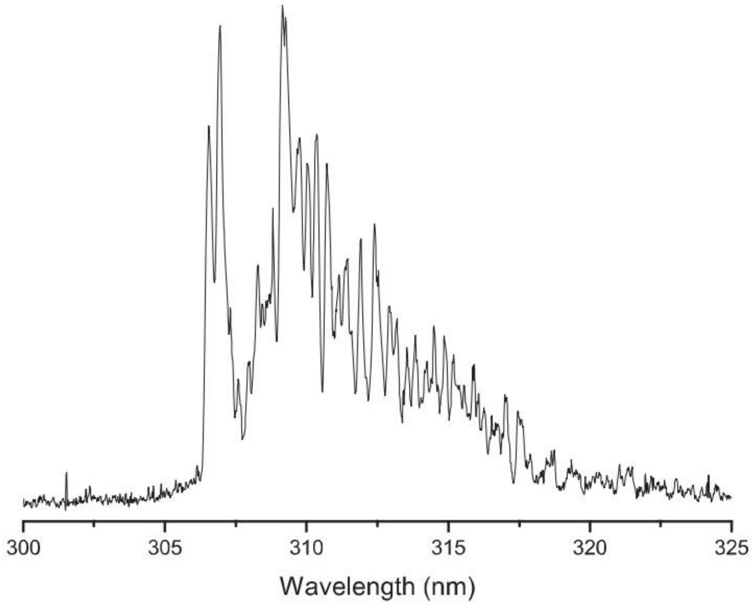

Figure 8. The molecular emission spectrum of OH [96]

Table 2. The wavelength ranges of all the molecules

Species	Wavelength (nm)	Ref.	Species	Wavelength (nm)	Ref.
CC	436.5	[95]	CH	431.5	[100]
	437.1			432.3	
	438.2			438.4	
	466.9			388.9	
	467.8			387.1	[101, 102]
	468.5			314.4	
	469.7	[96]		315.7	
	471.5		OH	306.4	[96]
	473.7			306.8	
	505.6			307.8	
	507.0			309.0	
	509.0			308.2	
	512.9			309.6	
	516.5	[107]	CN	358.6	[99]
	547.0			359.0	
	550.2			385.1	
	554.1			385.5	
	558.5			386.2	
	563.5			387.1	
	592.3			388.3	
	595.9			415.2	[79]
	600.5			415.6	
	606.0			416.8	
	619.1			418.1	
NH	336.3	[108]		419.7	
	337.4			421.6	

LIBS spectra through plasmas of organic matter may exhibit signals from fewer prominent species and emissions of organic substances like plastic. Nevertheless, the presence of these signals depends on the specific circumstances and analytical parameters [109]. The prominent aromatic compound is the C_3 radical, one of the most extensively researched triatomic molecules in spectroscopy. Its emissions have been detected in LIBS spectra of solid graphite microplasmas produced by an Nd: YAG laser beam such as 1.06 μm, 3.5 ns, 6.9 $J.cm^{-2}$ in a 0.5–415 mTorr argon background [110]. Neutral C_3 molecules emit a broad structure at 390–410 nm wavelength, which correlates to the Swings band transition (SBT) [111]. Empirical evidence has shown that the primary mode of C_3 production occurs in the gaseous state via three-body interactions involving carbon and carbon dioxide. It has been proven that using unfocused laser light is more advantageous for detecting neutral C_3 emission, primarily due to the reduced atomization process of the molecules [112].

Nevertheless, these emissions appear only in plasmas that expand into inert and N-free environments since there is a strong attraction between carbon and nitrogen to generate carbon nitride (CN). The N_2 radical is another potential species. The primary focus of optical emission spectroscopy has been on plasmas consisting of pure nitrogen gas and mixes of Ar-N_2 and N_2-He. It is perfectly feasible for N_2 molecular species to appear in laser-generated plasmas of azo and diazo compounds. However, there is a lack of references to these experiments conducted using optical emission spectroscopy. The emission spectrum typically corresponds to the approximate wavelength ranges of 268.0–546.0 nm and 478.0–2531.0 nm for the N_2 species and 205.0–307.0 nm and 286.0–587.0 nm for the N^{2+} species [113].

In any scenario, simultaneous detection of optical emissions from various emitting species within a LIBS spectrum is challenging due to numerous variables. These variables include the composition and bonding of atoms within the molecule, the fragmentation behaviour of the molecule, the timing and duration of plasma observation, whether in its entirety or within a specific spatial region, as well as the structure and reactivity of the environment around it. In addition, the presence of numerous species and the resulting variations in the intensity of their emissions, leading to periodic overlap between emissions, along with the utilization of a shorter wavelength measurement range to attain enhanced spectral resolution, further contribute to the challenge of achieving emissions coincidence. The factors mentioned above raise many questions about organic plasmas and chemical and physical phenomena, prompting extensive research to elucidate these phenomena.

According to the literature cited in this section and surveys, the range of synthetic organic polymers typically spans from approximately 350 to 700 nm. Consequently, during laser experimentation with plastics, it becomes convenient to focus within these ranges to analyze the spectrum or verify bond breakage. Additionally, this strategy enables control over experiments aimed at breaking specific bonds. For instance, when targeting the breaking of C-H bonds while avoiding C-C bonds, these spectra can assist in analyzing the phenomenon. If C-C bonds persist during spectrum collection, it indicates the presence of C-C bonds. However, it is not possible to control experimentation under nano-lasers.

8. Physics of plasma formation

This section will examine the formation route of species, their dynamics, the properties that they contribute to the resulting plasma, and the impact of experimental conditions.

Whenever a laser interacts with organic material, such as plastic, the intense laser beam transfers energy to the material, leading to decomposition and plasma formation. The material absorbs the light at this moment, causing electrons to be excited from lower to higher orbits. This phenomenon occurs within microseconds or nanoseconds, and the excited atoms return to their initial state by emitting light at specific wavelengths. During the life cycle of the plasma formed during laser ablation with plastic species, it undergoes simultaneously processed formation, evolution, and destruction. The laser irradiation parameters determine the generation of ions, atoms, elements, and nanoparticles. The factors influencing the quantity of ablated atoms from the organic bulk and how these molecules fragment include the excitation regime, laser wavelength, and energy dose. Generally, fragmentation processes are the main focus during femtosecond (fs) laser ablation, whereas atomization of vaporized molecules is the dominant process in the case of ns pulses. The energetic dose significantly influences the cause of ablation. Specifically, for low, middle, and high influence, the plasma mainly comprises large fragments, tiny molecules, and atoms **[**114].

Similarly, some bonds or clusters of bonds could be broken based on the wavelength of the laser, resulting in the formation of different species [115]. These recommendations expect that the quantity and characteristics of the species produced may differ significantly across different plasma plumes, even for an identical organic chemical. Nevertheless, there are instances when the collective influence of several factors produces comparable outcomes, such as a high fluence fs laser pulse compared to a lower fluence laser pulse but with a longer length (ns). In addition to the factors mentioned above, the initial species exhibit distinct spatial and temporal progression inside the plasma plume, influenced by their kinetics, characteristics, and the pressure of the surrounding atmosphere. Consequently, this phenomenon gives rise to several possibilities for generating novel species.

The physics of a plasma plume is transformed into a complicated process, including several participating and coexisting processes that influence its composition at various periods and localized areas. Therefore, it can be assumed from the information mentioned above that each variable contributes to the advancement of plasma. Still, their collective influence generates a specific sequence of events that eventually determine the characteristics and magnitude of the ultimate optical emissions.

9. The bond-breaking hypothesis of HDPE

9.1. Philosophical Background

This section briefly overviews the background and the underlying phenomenon involved in breaking the bonds of HDPE to facilitate laser-induced pyrolysis. For example, Thiele *et al.* [116] propose an ideology shift by challenging the generally accepted belief that rapid vibrational relaxation rates inside molecules restrict bond-breaking. The suggested model showed the specificity in bond breaking, which can be accomplished using appropriately short and intense laser pulses, opening up new paths for commercial-scale laser applications.

This study has considerable importance for the proposed HDPEbond breaking, as it intends to understand the behaviour of molecules and chemical interaction control via laser-induced processes. The significant breakthroughs in their research open the path for our investigation into using these particular bond-breaking technologies. While conducting more research on practical applications and optimization is crucial, this study serves as a valuable reference and source of inspiration. This study outlines the methodologies and objectives for the planned laser-induced cleavage of HDPE. The combination of insights on potential selective bond cleavage and a focus on ongoing research provides a strong basis. The laser pulse experiments investigate polyethene's molecular structures and properties at its core.

Similarly, Soleimani *et al*. [117] analyzed the possibility of selectively breaking polyethene connections by targeted ultrafast energy deposition inspired by comparable research on customized damage to semiconductor bonds. Hence, the examination of HDPE dissociation requires further exploration. A comprehensive exam has the potential to provide scientific knowledge and advancements in technology while also encouraging more investigations. The hypothetical discussion on conducting HDPE laser pyrolysis is given below.

The most significant component of bond breaking involves understanding the type of plastic and the bonds it includes, such as which bonds are present in the plastic and how much energy is necessary to break them. Another essential factor is the employment of a laser, which has sufficient energy to break the bonds in the plastic. The third step is to optimize process parameters such as pulse energy, pulse duration, and laser pulse repetition. For example, if the plastic type is HDPE, which is relatively easy to handle during experiments, the only bonds are C-C and C-H. 3.6 eV and 4.3 eV of energy would be required to break these bonds. A UV laser with a wavelength of 200-400 nm could be suitable to efficiently break the chemical bonds of HDPE, which can be confirmed by using the relation $E=\frac{hc}{\lambda}$. Here, E, h, c, and λ represent photon energy, Planck's constant, light speed, and light wavelength, respectively. This calculation indicates that UV radiation with a wavelength of 266 nm has enough photon energy to break molecular bonds in HDPE. However, the expected initial problem could be the laser's pulse duration due to the instant breaking of bonds. It could be probed by a laser at the femtosecond or pico-second pulse duration to overcome this situation.

9.2. Significance of process parameters

Optimizing laser process parameters, such as pulse power, duration, and frequency repetition rate, is pivotal for realizing experimental efficacy, as evidenced through extensive examination of laser-material interaction dynamics. The selection of pulse energy from 10-200 millijoules (mJ) can be supported by its critical function in facilitating effective HDPE removal and plasma constitution while preventing complex spectral generation and unnecessary material harm [118]. This energy range is considered from empirical reports denoting optimal ablation thresholds and plasma formation conditions for polymers similar to HDPE. The 5-20ns pulse duration is concise, which can produce high-resolution spectrum peaks with efficient plasma formation since a longer pulse duration from this limit can lead to plasma shielding and lower plasma efficiency [119]. A repetition frequency (Rf) of 20Hz could be a delicate balance between the speed of data collection and the need for sample cooling.

Moreover, the process parameter’s intensity selection depends on the specific focus or information required. This consideration becomes particularly relevant in UV laser interactions with HDPE, where reliance solely on cited literature may not be feasible. Under normal conditions, such as in traditional thermal pyrolysis, bond-breaking behaviour is determined by bond dissociation energy and bond length, leading to the initial breaking of C-C bonds. However, this dynamic may not be valid under UV laser application to HDPE. It becomes essential to consider absorption and vibrational effects. Logically, it would appear that C-C bonds should break before C-H bonds due to their lower energy requirements and longer bond lengths, as illustrated in Figure 9. However, according to the hypothetical point of view of the UV laser exposure to HDPE, it is posited that C-H bonds would break first, given their heightened sensitivity to light, similar to sunlight exposure. Another contributing factor is the difference in electronegativity between the two types of bonds. The C-C bonds are non-polar, whereas the C-H bonds are polar. This means that the energy of photons emitted by the UV laser is likely similar to the energy required to excite the electrons in C-H bonds.

Additionally, the energy difference between breaking C-C bonds, which require 3.6 eV, and C-H bonds, which require 4.2 eV, is not substantial. Owing to this sensitivity, C-H bonds are more likely to absorb UV light than C-C bonds, resulting in greater vibration and an increased likelihood of breaking. It is also possible that under UV irradiation, the C-H bonds initially break, but the overall majority of breaking might involve C-C bonds. Anyway, this outcome still depends on the intensity of the process parameters. However, the behaviour of plasma remains complex; it could also lead to decomposition over time, which may be influenced by the intensity of the process parameters that can modify the plasma's effects. In this context, it is crucial to consider the implications of UV interaction, such as the effects of direct photon absorption. The possible questions could be: Will increased photon absorption cause extensive vibration? Can this vibration lead to excitation, and in turn, does excitation lead to a collision, ultimately resulting in the initial breaking of C-H bonds? This complexity could be solved after understanding the role of process parameters.

The frequency may be the most crucial among all the process parameters, as it is essential for breaking bonds. Pulse duration could be considered the second most vital factor, as different processes occur with varying pulse durations, for example, between ns and fs laser pulses. Therefore, experiments must be conducted to observe how bonds react under different light exposure conditions to determine the optimal combination of process parameters.

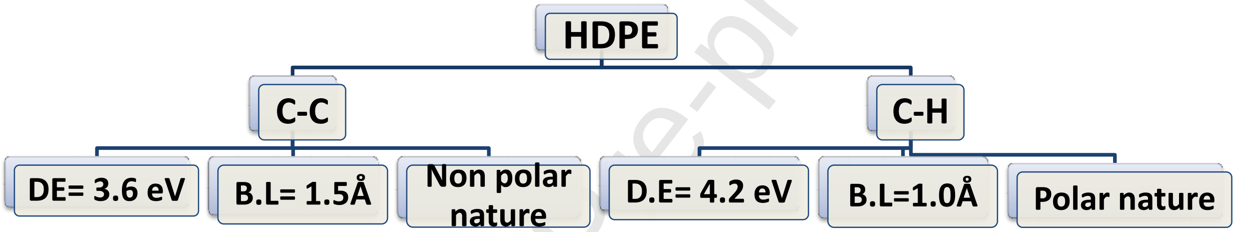

Figure 9. The graphical overview provides bonding information for HDPE. 'DE' refers to dissociation energy, and 'BL' refers to bond length.

9.3. Selection of HDPE form

The choice of HDPE in a particular form, such as film, pellet, sheet, or block, is a critical decision with far-reaching implications for the experiment's result. In the framework of a bond-breaking investigation, the film form option could be the best choice. Despite its thickness (10-100 micrometres), the film shape allows for studying surface interactions, resulting in a more detailed understanding of the early bond-breaking effects. This possibility is consistent with a desire to thoroughly understand how the laser interacts with HDPE at the molecular level and how the bonds break. However, all types of HDPE might be studied under similar experimental conditions to identify the most effective strategy.

9.4. Precautions

A precise sample holder is necessary for ensuring HDPE samples' stability and proper alignment with the laser. Equipment calibration, such as accurate laser alignment with the material being studied and adjusting the spectrometer for recording the plasma spectrum, is essential for reliable and precise information collection. Safety protocols, including protective eyewear, a covered laser area, and enough ventilation to control fumes or vapours, reveal a commitment to the experiment's protection and achievement. Remembering that this study is only valid under vacuum conditions is critical. The predominant impact of radiation from lasers on HDPE in open air could be the breakdown of existing polymer links. However, under some circumstances, new bonds containing oxygen or, less commonly, nitrogen can form. The reliable outcomes would be determined by experimental setup, including the laser's power, wavelength, and exposure time.

9.5. Expectations

Beyond the technical details, understanding how the UV laser affects HDPE at the molecular level is critical for unravelling the bond-breaking process. Correlating experimental findings to theoretical expectations for bond energies and HDPE behaviour under high-energy UV radiation takes the study to a new level of exploration. This association serves as the key to unlocking a comprehensive knowledge of the specific point of modification in the molecular structure of HDPE under the effect of LIBS. In line with this, this understanding will also enable us to take a look into the conducting of HDPE pyrolysis-assisted LIBS, which has been discussed in detail in the next section. Tables 3 and 4 summarize the expected ranges of process parameters as well as the benefits and drawbacks of experimental prediction.

Table 3. The expected ranges of process parameters for 266 nm laser

Laser Setup	
Laser range	266 nm (4.66eV)
Pulse duration	5-20ns
Pulse Energy	10-200 mJ
Frequency Rep.	1-20Hz
Plano-convex Lens	30 cm
Spectrometer	CCD-Coupled
Optical Fiber	190-770 nm
Resolution	0.05 nm

Table 4. Expectations of the experiment with advantages and drawbacks

HDPE form	Advantages	Drawbacks	Expectations
Film (10-100 μm)	Surface interactions study	Thickness will limit observation	Clear view of how the laser interacts with the material at the molecular level
Pellet (2-5 mm)	Thermal and mechanical study	Small surface area	How will laser energy affect HDPE?
Sheet (0.5-2 mm)	Larger and more uniform area	Low penetration and thicker	Will it reveal how deep the bond-breaking penetrates?
Note that C-C bonds require 3.6eV energy to break, and C-H bonds require 4.3eV energy to break.			

A different approach for HDPE bond breaking is using a laser (IR or Raman), which only analyses the frequencies without relying on the reference spectrum. When the laser frequency is much higher than the bond frequency, the solid HDPE will transform into its gaseous form, most probably leading to methane (CH_4) gas [120]. It's important to highlight that introducing a catalyst can also modify the final products[121-123]. The presence of the gas could be identified using a gas analyzer, which will verify the degradation of the HDPE bond. For instance, the approximate frequency of a single bond is often between 800-1300 cm^{-1}. If we examine a gas using a particular wavelength with a frequency much higher than the bond frequency, we may detect the breaking of the bonds using a gas analyzer. It should be noted that the minimum frequency or repetition rate depends on the type of laser being utilized, such as nanosecond (ns), femtosecond (fs), or CO_2 lasers. Consequently, the frequency must obey the principles governing dissociation processes.

9.6. The hypothesis of Laser-Induced HDPE Pyrolysis

This section presents an overview of the hypothesis for conducting HDPE pyrolysis using a laser. According to the literature, LIBS is primarily used for elemental analysis, in which light of a certain wavelength is utilized to excite the sample's surface, resulting in plasma, to get information about the elemental composition or identification. This phenomenon is particularly dependent on the range of light or wavelength and energy. On the other hand, pyrolysis refers to the breakdown of any substance in the absence of oxygen to estimate the ultimate yields, including oil, gas, waxes, and so on [124-132]. A specific temperature has to be established, which requires energy [133-138]

The previous section discussed how to compute photons' exact wavelength and energy using a laser to break HDPE bonds. At this time, it is theoretically possible to employ a laser to decompose HDPE in a reactor. A continuous particular wavelength of light with sufficient energy of 1.44×10^{22}eV could decompose C-C bonds. Depending on the kind of light, CO_2 Lasers (10.6 μm), Nd: YAG Lasers (1064 nm), Fiber Lasers (1060-1080 nm), and femtosecond Ti: sapphire lasers (800 nm) could produce this energy. It should be noted that before the experiment, other factors such as reactor type, HDPE size, frequency factor, and pulse duration should be taken into consideration.

According to this hypothesis, precise control of laser wavelengths and energy could offer thermal pyrolysis. It is feasible to achieve the necessary results. Nevertheless, it will not be more effective for large-scale recycling. So that the hypothesis could be considered for further investigation if there is a possible or suitable way to perform this investigation after improvements. In summary, if we can identify a specific collection of wavelengths that are favourably associated with a combination of process parameters, it may be feasible to use a laser for performing the pyrolysis of HDPE. Currently, this theory requires additional attention and investigation.

9.7. Selection of Environment

Plasma can be created in both air and vacuum, depending on the aim of the research study. Generating plasma in a vacuum significantly reduces the presence of air contaminants, leading to enhanced spectral clarity. It offers a reasonable control area enabling the examination of components that may interact with environmental molecules or detect contaminants. Additionally, these control conditions provide a better insight into the interaction of laser and materials, enhancing spectral detection of light elements [139]. It has the potential to prolong the presence of plasma, allowing for a longer emission duration for triggered kinds and enhancing the detection limitations and precision of the inspection.

Initially, conducting this experiment in the open air is easier since a vacuum can cause complexities when employing LIBS with HDPE. Adding a chamber could increase the cost, and the sample size may not be adjustable. Placing samples in a vacuum may significantly limit the size and characteristics of materials that can be examined. The effects of energy transfer processes on outcomes may subtly vary when air particles are absent in the surrounding environment.

10. Drawbacks and Expectations of Hypothesis:

One potential question that may arise involves the difference in efficiency between conventional (thermal) and laser-induced pyrolysis. This aspect can be regarded as an initial limitation of the hypothesis, as it remains indeterminable until an experiment is conducted [140-142]. After obtaining the experimental data, two possible approaches can optimize the hypothetical process. The first involves implementing machine learning models to analyze hidden spectra or signals and address the fundamental causes of bond-breaking phenomena to optimize the initial process parameters (pulse energy, duration, wavelength range, and frequency factors). Alongside machine learning approaches, mathematical or semi-empirical models can be utilized to extract reaction formation routes and empirical kinetic rate constants. This enables the reverse-engineering of observed phenomena, optimising secondary process parameters (rate constants, activation energy, exponential factor, temperature, type of reactor, etc.) involved in laser-induced HDPE pyrolysis [143-151]. It is important to note that both traditional and laser pyrolysis rely on the reaction scheme and kinetic rate constants, which serve as the foundation for analyzing the final yield in pyrolysis. The method for obtaining kinetic rate constants can involve extracting them from empirical data using Runge Kutta-based solvers in MATLAB or predicting them using statistical approaches, depending on the preference.

Additionally, different statistical approaches are used to predict statistical rate constants. This technique examines the reaction process and estimates the ultimate yield. Following this, a detailed validation of the kinetic rate constants involves conducting sensitivity analyses for each rate constant. This approach allows for examining how each rate constant influences the final yield as a function of time and temperature. For example, Eidesen *et al*. [143] extracted empirical rate constants from experimental data and designed a mathematical model using the second-order differential (ODE) equation to simulate the final yield. Nabi *et al*. [152] employed a regression model to predict the rate constants using R software statistically.

Similarly, Alqarni *et al*. [153] used R software to predict statistical rate constants by statistically assuming a correlated combination of activation energy (Ea) and exponential factor (Ao). Irfan *et al*. [146] predicted statistical rate constants by employing the response surface methodology using Ea and Ao. Additionally, Irfan *et al*. [154, 155] performed sensitivity analyses of predicted rate constants to examine the individual behaviour of kinetic rate constants, using lower and higher extreme levels as conditions.

The literature cited above provides evidence for the extraction of empirical and prediction of statistical rate constants and sensitivity analysis using various mathematical and statistical approaches. It is clear that most approaches in the cited literature are mathematical or semi-empirical, always necessitating an initial equation and condition to analyze the final yield. This analysis helps gain insight into the underlying processes and identifies potential modifications for enhancing the efficiency of laser-induced HDPE pyrolysis. Figure 10 serves as a roadmap, guiding the journey from the initial to the final stage through a combination of experimentation and simulation approaches toward utilising data that could be obtained from experimentation.

It should also be noted that thermal pyrolysis is highly inefficient, yet it can be sustained by by-products such as CH_4 [150, 151]. However, the by-products cannot be utilized for sustainability in laser-induced pyrolysis. During laser-induced pyrolysis, the primary outputs will be gaseous products rather than petroleum products, which rely on specific conditions. Nevertheless, laser-induced ionization may exhibit higher efficiency in hydrocarbon extraction from HDPE, and the whole procedure may have environmental benefits. The implementation of the direct energy supply system may result in a decrease in the total energy consumption. The fast interaction between laser and HDPE may decrease pyrolysis reaction time, and therefore, the localized nature of laser-induced pyrolysis reaction may be energy efficient. Laser-induced pyrolysis can optimize chemical reactions, i.e., selectivity to target C-C or C-H bonds. This control may save energy and time, leading to environmental advantages. The laser pyrolysis process may also have fewer by-products/waste than thermal pyrolysis, reducing the overall HDPE recycling carbon footprint.

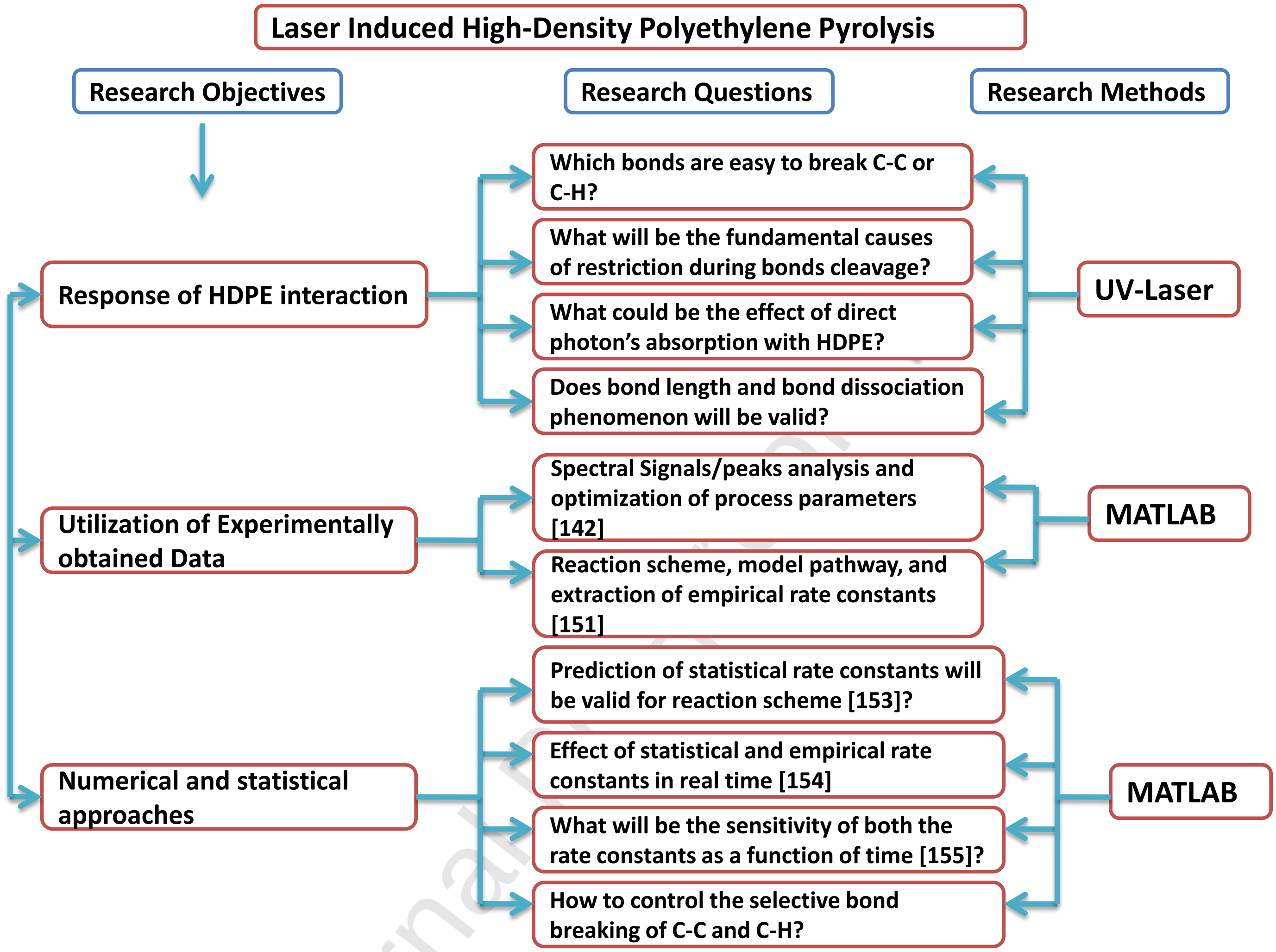

Figure 10. The optimization roadmap of laser-induced HDPE pyrolysis

Conclusion

LIBS is extensively used to identify atoms, ions, and molecules and their emission characteristics under different conditions. Different supervised and unsupervised models and machine learning were employed for the plastic sorting, classification, and composition analysis. However, a brief overview of the cited literature reveals that LIBS has not been utilized to understand plastic behaviour by applying enough energy to break the chemical composition of materials to understand the chemistry of actual materials and new chemical formation. To enhance the recycling quality of plastic, it is imperative to understand the mechanism of the interaction of lasers with plastic at the molecular level. During commercial-scale recycling, it is possible to categorize, identify, and sort the plastic to obtain the end product; however, the contradiction between the cited and actual findings insists on looking into the exact cause. The possible reason behind this is the phenomenon of plastic degradation during recycling under high-energy lasers. It is imperative to understand what plastic bonds are feasible to break. What kind of bonds are not breakable, and why? According to the aforementioned details in section 9, it could be possible to analyze the bond-breaking behaviour by ensuring the law of degradation (Laser photon energy must be higher than the bond energy) with modification in the intensity of process parameters.

This direction can lead toward the fundamental causes that happen during recycling. There could be a lot of difficulties during the collection of spectrum data; however, a problem can be caused by a solution that will open new paths and ideas to overcome this research gap. The critical characteristics of pyrolysis are the kinetic rate constants and yield concentration that could be obtained from the LIBS experiment data. If the traditional LIBS is unable to achieve this goal, the ultrafast LIBS could allow the performing of a control experiment. Laser pyrolysis could also be achieved if a positively correlated combination of involved LIBS process parameters for HDPE bond-breaking.

Acknowledgements

This work was in part supported by NSAF (Grant No. U2130123), the Shanghai Science and Technology Program (Grant No.21511105000), and the International Partnership Program of the Chinese Academy of Sciences (Grant No. 181231KYSB20200033). Rao Adeel Un Nabi acknowledges the CSC Scholarship for International Students.

References

[1] P. Das, P. Tiwari, J.M. Lee, 2024. Multistep kinetic analysis of additive-enhanced plastic degradation. Chemical Engineering Journal. 488, 150960. https://doi.org/10.1016/j.cej.2024.150960.

[2] P. Shi, T. Huang, H.K. Lim, C.K. Tan, J.M. Lee, C.Y. Tay, 2024. Transforming electronic plastics into bioadaptive 3D porous construct for advanced cell culture applications. Resources, Conservation and Recycling. 200, 107297. https://doi.org/10.1016/j.resconrec.2023.107297

[3] P. Das, Q. Zeng, A. Leybros, J.C.P. Gabriel, C.Y. Tay, J.M. Lee, 2023. Enhanced extraction of brominated flame retardants from e-waste plastics. Chemical Engineering Journal. 469, 144126. https://doi.org/10.1016/j.cej.2023.144126

[4] P. Shi, C.K. Tan, Z. Wu, J.C.P. Gabriel, M. Srinivasan, J.M. Lee, C.Y. Tay, 2022. Direct reuse of electronic plastic scraps from computer monitor and keyboard to direct stem cell growth and differentiation. Science of The Total Environment. 807, 151085. https://doi.org/10.1016/j.scitotenv.2021.151085

[5] Y. Wan, Q. Zeng, P. Shi, Y.J. Yoon, C.Y. Tay, J.M. Lee, 2022. Machine learning-assisted optimization of TBBPA-bis-(2, 3-dibromopropyl ether) extraction process from ABS polymer. Chemosphere. 287, 132128. https://doi.org/10.1016/j.chemosphere.2021.132128

[6] C. Jia, P. Das, I. Kim, Y.J. Yoon, C.Y. Tay, J.M. Lee, 2022. Applications, treatments, and reuse of plastics from electrical and electronic equipment. Journal of Industrial and Engineering Chemistry. 110, 84-99. https://doi.org/10.1016/j.jiec.2022.03.026

[7] Y. Wan, Q. Zeng, I. Kim, P. Shi, Y.J. Yoon, C.Y. Tay, J.M. Lee, 2022. Ultrasonic-assisted tetrabromobisphenol A-bis-(2, 3-dibromo-2-methylpropyl ether) extraction process from ABS polymer supported by machine learning. Environmental Technology & Innovation. 27, 102485. https://doi.org/10.1016/j.eti.2022.102485

[8] C. Jia, P. Das, Q. Zeng, J.C.P. Gabriel, C.Y. Tay, J.M. Lee, 2022. Activated recovery of PVC from contaminated waste extension cord-cable using a weak acid. Chemosphere. 303, 134878. https://doi.org/10.1016/j.chemosphere.2022.134878

[9] K. Li, Y. Wang, W. Zhou, T. Cui, J. Yang, Z. Sun, Y. Min, J.M. Lee, 2022. Catalytic pyrolysis of film waste over Co/Ni pillared montmorillonites towards H2 production. Chemosphere. 299, 134440. https://doi.org/10.1016/j.chemosphere.2022.134440

[10] P. Shi, Y. Wan, A. Grandjean, J.M. Lee, C.Y. Tay, 2021. Clarifying the in-situ cytotoxic potential of electronic waste plastics. Chemosphere. 269, 128719. https://doi.org/10.1016/j.chemosphere.2020.128719

[11] P. Das, J.C.P. Gabriel, C.Y. Tay, J.M. Lee, 2021. Value-added products from thermochemical treatments of contaminated e-waste plastics. Chemosphere. 269, 129409. https://doi.org/10.1016/j.chemosphere.2020.129409

[12] D. Xia, A. Maurice, A. Leybros, J.M. Lee, A. Grandjean, J.C.P. Gabriel, 2021. On-line spectroscopic study of brominated flame retardant extraction in supercritical CO2. Chemosphere. 263, 128282. https://doi.org/10.1016/j.chemosphere.2020.128282

[13] W.K. Yahya, N.D. Musa, N.H. Hashim, 2016. Understanding environmentally friendly consumer behavior. In Regional Conference on Science, Technology and Social Sciences (RCSTSS 2014) Business and Social Sciences. Springer Singapore. pp. 909-921. https://doi.org/10.1007/978-981-10-1458-1_82

[14] J.L. Baker, ed., 2012. Climate change, disaster risk, and the urban poor: cities building resilience for a changing world. World Bank Publications. https://doi.org/10.1596/978-0-8213-8845-7

[15] S. Fletcher, A.L.A. March, K. Roberts, Y. Shirian, L.M. i Canals, A. Cairns, P. Lefort, A. Meso, A.D. Raine, A. Smagadi, S. Stone, 2023. Turning off the Tap: How the world can end plastic pollution and create a circular economy. United Nations Environment Programme. https://doi.org/10.59117/20.500.11822/42277

[16] M.M. Ahmed, A.W. Elawadly, M.A. Gohary, 2023. The Role Of Urban Sustainability Mechanisms In Raising The Efficiency And Organization Of Urban Management in Egyptian Cities, A Case Study (El-Salam District, Port Said). Port-Said Engineering Research Journal. 27(2), 23-39. https://doi.org/10.21608/pserj.2023.193624.1220

[17] S. Lazăr, D. Dobrotă, R.E. Breaz, S.G. Racz, 2023. Eco-Design of Polymer Matrix Composite Parts: A Review. Polymers. 15(17), 3634. https://doi.org/10.3390/polym15173634

[18] R. Van Berkel, 2007. Cleaner production and eco-efficiency initiatives in Western Australia 1996–2004. Journal of Cleaner production. 15(8-9), 741-755. https://doi.org/10.1016/j.jclepro.2006.06.012

[19] I. Lorenzoni, S. Nicholson-Cole, L. Whitmarsh, 2007. Barriers perceived to engaging with climate change among the UK public and their policy implications. Global environmental change. 17(3-4), 445-459. https://doi.org/10.1016/j.gloenvcha.2007.01.004

[20] V. Beghetto, V. Gatto, R. Samiolo, C. Scolaro, S. Brahimi, M. Facchin, A. Visco, 2023. Plastics today: Key challenges and EU strategies towards carbon neutrality: A review. Environmental Pollution. 122102. https://doi.org/10.1016/j.envpol.2023.122102

[21] I.A. Ignatyev, W. Thielemans, B. Vander Beke, 2014. Recycling of polymers: a review. ChemSusChem. 7(6), 1579-1593. https://doi.org/10.1002/cssc.201300898

[22] M.Y. Khalid, Z.U. Arif, W. Ahmed, H. Arshad, 2022. Recent trends in recycling and reusing techniques of different plastic polymers and their composite materials. Sustainable Materials and Technologies. 31, e00382. https://doi.org/10.1016/j.susmat.2021.e00382

[23] B.D. Vogt, K.K. Stokes, S.K. Kumar, 2021. Why is recycling of postconsumer plastics so challenging?. ACS Applied Polymer Materials. 3(9), 4325-4346. https://doi.org/10.1021/acsapm.1c00648

[24] X. Jiang, B. Zhu, M. Zhu, 2023. An Overview on Recycling of Waste Poly (Vinyl Chloride). Green Chemistry. https://doi.org/10.1039/d3gc02585c

[25] R. Zuo, Y. Xiong, J. Wang, E.J.M. Carranza, 2019. Deep learning and its application in geochemical mapping. Earth-science reviews. 192, 1-14. https://doi.org/10.1016/j.earscirev.2019.02.023

[26] T. Chen, T. Zhang, H. Li, 2020. Applications of laser-induced breakdown spectroscopy (LIBS) combined with machine learning in geochemical and environmental resources exploration. TrAC Trends in Analytical Chemistry. 133, 116113. https://doi.org/10.1016/j.trac.2020.116113

[27] K. Palanivel, J. Varghese, 2024. Laser-induced breakdown spectroscopy with neural network approach for plastic identification and classification in waste management. Applied Chemical Engineering. 7(1). https://doi.org/10.24294/ace.v7i1.3092

[28] H.K. Imhof, J. Schmid, R. Niessner, N.P. Ivleva, C. Laforsch, 2012. A novel, highly efficient method for the separation and quantification of plastic particles in sediments of aquatic environments. Limnology and oceanography: methods. 10(7), 524-537. https://doi.org/10.4319/lom.2012.10.524

[29] V. Hidalgo-Ruz, L. Gutow, R.C. Thompson, M. Thiel, 2012. Microplastics in the marine environment: a review of the methods used for identification and quantification. Environmental science & technology. 46(6), 3060-3075. https://doi.org/10.1021/es2031505

[30] J.D. Pedarnig, S. Trautner, S. Grünberger, N. Giannakaris, S. Eschlböck-Fuchs, J. Hofstadler, 2021. Review of element analysis of industrial materials by in-line laser—induced breakdown spectroscopy (LIBS). Applied Sciences. 11(19), 9274. https://doi.org/10.3390/app11199274

[31] A. Bellasi, G. Binda, A. Pozzi, G. Boldrocchi, R. Bettinetti, 2021. The extraction of microplastics from sediments: An overview of existing methods and the proposal of a new and green alternative. Chemosphere. 278, 130357. https://doi.org/10.1016/j.chemosphere.2021.130357

[32] S. Primpke, S.H. Christiansen, W. Cowger, H. De Frond, A. Deshpande, M. Fischer, E.B. Holland, M. Meyns, B.A. O'Donnell, B.E. Ossmann, M. Pittroff, 2020. Critical assessment of analytical methods for the harmonized and cost-efficient analysis of microplastics. Applied Spectroscopy. 74(9), 1012-1047. https://doi.org/10.1177/0003702820921465

[33] V. Beghetto, R. Sole, C. Buranello, M. Al-Abkal, M. Facchin, 2021. Recent advancements in plastic packaging recycling: A mini-review. Materials. 14(17), 4782. https://doi.org/10.3390/ma14174782

[34] H.C. Erythropel, J.B. Zimmerman, T.M. de Winter, L. Petitjean, F. Melnikov, C.H. Lam, A.W. Lounsbury, K.E. Mellor, N.Z. Janković, Q. Tu, L.N. Pincus, 2018. The Green ChemisTREE: 20 years after taking root with the 12 principles. Green Chemistry. 20(9), 1929-1961. https://doi.org/10.1039/c8gc00482j

[35] V. Beghetto, R. Sole, C. Buranello, M. Al-Abkal, M. Facchin, 2021. Recent Advancements in Plastic Packaging Recycling: A Mini-Review. Materials. 14(17), 4782. https://doi.org/10.3390/ma14174782

[36] J. Singh, R. Kumar, S. Awasthi, V. Singh, A.K. Rai, 2017. Laser Induced breakdown spectroscopy: A rapid tool for the identification and quantification of minerals in cucurbit seeds. Food Chemistry. 221, 1778-1783. https://doi.org/10.1016/j.foodchem.2016.10.104

[37] R. Junjuri, C. Zhang, I. Barman, M.K. Gundawar, 2019. Identification of post-consumer plastics using laser-induced breakdown spectroscopy. Polymer Testing. 76, 101-108. https://doi.org/10.1016/j.polymertesting.2019.03.012

[38] V.C. Costa, J.P. Castro, D.F. Andrade, D.V. Babos, J.A. Garcia, M.A. Sperança, T.A. Catelani, E.R. Pereira-Filho, 2018. Laser-induced breakdown spectroscopy (LIBS) applications in the chemical analysis of waste electrical and electronic equipment (WEEE). TrAC Trends in Analytical Chemistry. 108, 65-73. https://doi.org/10.1016/j.trac.2018.08.003

[39] D.J. Malenfant, A.E. Paulick, S.J. Rehse, 2019. A simple and efficient centrifugation filtration method for bacterial concentration and isolation prior to testing liquid specimens with laser-induced breakdown spectroscopy. Spectrochimica Acta Part B: Atomic Spectroscopy. 158, 105629. https://doi.org/10.1016/j.sab.2019.05.018

[40] Q. Wang, X. Cui, G. Teng, Y. Zhao, K. Wei, 2020. Evaluation and improvement of model robustness for plastics samples classification by laser-induced breakdown spectroscopy. Optics & Laser Technology. 125, 106035. https://doi.org/10.1016/j.optlastec.2019.106035

[41] M. Król, K. Gondko, A. Kula, P. Własiuk, J.M. del Hoyo-Meléndez, P. Kościelniak, 2020. Characterization of the elemental composition of Polish banknotes by X-ray fluorescence and

laser-induced breakdown spectroscopy. Spectrochimica Acta Part B: Atomic Spectroscopy. 169, 105898. https://doi.org/10.1016/j.sab.2020.105898

[42] Y. Tang, Y. Guo, Q. Sun, S. Tang, J. Li, L. Guo, J. Duan, 2018. Industrial polymers classification using laser-induced breakdown spectroscopy combined with self-organizing maps and K-means algorithm. Optik. 165, 179-185. https://doi.org/10.1016/j.ijleo.2018.03.121

[43] D. Chen, T. Wang, Y. Ma, G. Wang, Q. Kong, P. Zhang, R. Li, 2020. Rapid characterization of heavy metals in single microplastics by laser induced breakdown spectroscopy. Science of The Total Environment. 743, 140850. https://doi.org/10.1016/j.scitotenv.2020.140850

[44] L. Brunnbauer, S. Larisegger, H. Lohninger, M. Nelhiebel, A. Limbeck, 2020. Spatially resolved polymer classification using laser induced breakdown spectroscopy (LIBS) and multivariate statistics. Talanta. 209, 120572. https://doi.org/10.1016/j.talanta.2019.120572

[45] Y. Liu, F. Yin, T.J. Wang, Y. Leng, R. Li, Z. Xu, S.L. Chin, 2024. Stable, intense supercontinuum light generation at 1 kHz by electric field assisted femtosecond laser filamentation in air. Light: Science & Applications. 13(1), 42. https://doi.org/10.1038/s41377-023-01364-3

[46] F. Yin, T.J. Wang, Y. Liu, J. Long, Y. Wei, B. Zhu, K. Zhou, Y. Leng, 2024. Pulse repetition rate effect on the plasma inside femtosecond laser filament in air. Chinese Optics Letters. 22(1), 013201. https://doi.org/10.3788/col202422.013201

[47] X. Peng, B. Xu, Z. Xu, X. Yan, N. Zhang, Y. Qin, Q. Ma, J. Li, N. Zhao, Q. Zhang, 2021. Accuracy improvement in plastics classification by laser-induced breakdown spectroscopy based on a residual network. Optics Express. 29(21), 33269-33280. https://doi.org/10.1364/oe.438331

[48] D.W. Hahn, N. Omenetto, 2010. Laser-induced breakdown spectroscopy (LIBS), part I: review of basic diagnostics and plasma–particle interactions: still-challenging issues within the analytical plasma community. Applied spectroscopy. 64(12), 335A-366A. https://doi.org/10.1366/000370210793561691

[49] T.A. Labutin, V.N. Lednev, A.A. Ilyin, A.M. Popov, 2016. Femtosecond laser-induced breakdown spectroscopy. Journal of Analytical Atomic Spectrometry. 31(1), 90-118. https://doi.org/10.1039/c5ja00301f

[50] S.K.H. Shah, J. Iqbal, P. Ahmad, M.U. Khandaker, S. Haq, M. Naeem, 2020. Laser induced breakdown spectroscopy methods and applications: A comprehensive review. Radiation physics and chemistry. 170, 108666. https://doi.org/10.1016/j.radphyschem.2019.108666

[51] S.N. Thakur, J.P. Singh, 2020. Fundamentals of LIBS and recent developments. Laser-Induced Breakdown Spectroscopy. 3-22. https://doi.org/10.1016/b978-0-12-818829-3.00001-0

[52] F.J. Fortes, J. Moros, P. Lucena, L.M. Cabalín, J.J. Laserna, 2013. Laser-induced breakdown spectroscopy. Analytical Chemistry. 85(2), 640-669. https://doi.org/10.1021/ac303220r

[53] J.D. Pedarnig, S. Trautner, S. Grünberger, N. Giannakaris, S. Eschlböck-Fuchs, J. Hofstadler, 2021. Review of element analysis of industrial materials by in-line laser—induced breakdown spectroscopy (LIBS). Applied Sciences. 11(19),9274. https://doi.org/10.3390/app11199274

[54] D. Holub, D.J. Palásti, K. Fintór, P. Pořízka, G. Galbács, J. Kaiser. Classification of Diverse Plastic Samples by Libs and Raman Data Fusion. Available at SSRN 4735153. https://doi.org/10.2139/ssrn.4735153

[55] E.R.K. Neo, J.S.C. Low, V. Goodship, S.R. Coles, K. Debattista, 2023. Development of a polymer spectral database for advanced chemometric analysis. Procedia CIRP. 116, 197-202. https://doi.org/10.1016/j.procir.2023.02.034

[56] J. Yang, Y.P. Xu, P. Chen, J.Y. Li, D. Liu, X.L. Chu, 2023. Combining spectroscopy and machine learning for rapid identification of plastic waste: Recent developments and future prospects. Journal of Cleaner Production. 139771. https://doi.org/10.1016/j.jclepro.2023.139771

[57] P.M. Anger, E. von der Esch, T. Baumann, M. Elsner, R. Niessner, N.P. Ivleva, 2018. Raman microspectroscopy as a tool for microplastic particle analysis. TrAC Trends in Analytical Chemistry. 109, 214-226. https://doi.org/10.1016/j.trac.2018.10.010

[58] G. Liu, D. Zhu, W. Zhou, S. Liao, J. Cui, K. Wu, D. Hamilton, 2010. Solid-phase photocatalytic degradation of polystyrene plastic with goethite modified by boron under UV–vis light irradiation. Applied Surface Science. 256(8), 2546-2551. https://doi.org/10.1016/j.apsusc.2009.10.102

[59] M. Doğan, 2021. Ultraviolet light accelerates the degradation of polyethylene plastics. Microscopy Research and Technique. 84(11), 2774-2783. https://doi.org/10.1002/jemt.23838

[60] G. Bonifazi, L. Fiore, P. Hennebert, S. Serranti, 2020. Development of a selection system based on hyperspectral imaging for plastic waste with brominated flame retardants. Environmental Engineering & Management Journal (EEMJ). 19(10). https://doi.org/10.30638/eemj.2020.166

[61] I. Barra, S.M. Haefele, R. Sakrabani, F. Kebede, 2021. Soil spectroscopy with the use of chemometrics, machine learning and pre-processing techniques in soil diagnosis: Recent advances–A review. TrAC Trends in Analytical Chemistry. 135, 116166. https://doi.org/10.1016/j.trac.2020.116166

[62] T.W. Wu, H. Zhang, W. Peng, F. Lü, P.J. He, 2023. Applications of convolutional neural networks for intelligent waste identification and recycling: A review. Resources, Conservation and Recycling. 190, 106813. https://doi.org/10.1016/j.resconrec.2022.106813

[63] D. Stefas, N. Gyftokostas, E. Bellou, S. Couris, 2019. Laser-induced breakdown spectroscopy assisted by machine learning for plastics/polymers identification. Atoms. 7(3), 79. https://doi.org/10.3390/atoms7030079

[64] Q. Duan, J. Li, 2021. Classification of common household plastic wastes combining multiple methods based on near-infrared spectroscopy. ACS ES&T Engineering. 1(7), 1065-1073. https://doi.org/10.1021/acsestengg.0c00183

[65] L. Pieszczek, M. Daszykowski, 2019. Improvement of recyclable plastic waste detection–A novel strategy for the construction of rigorous classifiers based on the hyperspectral images. Chemometrics and Intelligent Laboratory Systems. 187, 28-40. https://doi.org/10.1016/j.chemolab.2019.02.009

[66] D.J.D. Silva, H. Wiebeck, 2019. Predicting LDPE/HDPE blend composition by CARS-PLS regression and confocal Raman spectroscopy. Polímeros. 29, e2019010. https://doi.org/10.1590/0104-1428.00218

[67] S. Zhu, H. Chen, M. Wang, X. Guo, Y. Lei, G. Jin, 2019. Plastic solid waste identification system based on near infrared spectroscopy in combination with support vector machine. Advanced Industrial and Engineering Polymer Research. 2(2), 77-81. https://doi.org/10.1016/j.aiepr.2019.04.001

[68] F.M. Riese, S. Keller, 2020. Supervised, semi-supervised, and unsupervised learning for hyperspectral regression. Hyperspectral image analysis: Advances in machine learning and signal processing. 187-232. https://doi.org/10.1007/978-3-030-38617-7_7

[69] M. Alloghani, D. Al-Jumeily, J. Mustafina, A. Hussain, A.J. Aljaaf, 2020. A systematic review on supervised and unsupervised machine learning algorithms for data science. Supervised and unsupervised learning for data science. 3-21. https://doi.org/10.1007/978-3-030-22475-2_1

[70] T. Delgado, J.M. Vadillo, J.J. Laserna, 2018. Isomer discrimination in condensed phase by laser-induced breakdown spectrometry and laser-ionization mass spectrometry using a tailored paired-pulse excitation scheme. Journal of Analytical Atomic Spectrometry. 33(9), 1469-1476. https://doi.org/10.1039/c8ja00106e

[71] V.K. Unnikrishnan, K.S. Choudhari, S.D. Kulkarni, R. Nayak, V.B. Kartha, C. Santhosh, 2013. Analytical predictive capabilities of laser induced breakdown spectroscopy (LIBS) with principal component analysis (PCA) for plastic classification. RSC Advances. 3(48), 25872-25880. https://doi.org/10.1039/c3ra44946g

[72] K.M. Shameem, K.S. Choudhari, A. Bankapur, S.D. Kulkarni, V.K. Unnikrishnan, S.D. George, V.B. Kartha, C. Santhosh, 2017. A hybrid LIBS–Raman system combined with chemometrics: an efficient tool for plastic identification and sorting. Analytical and Bioanalytical Chemistry. 409, 3299-3308. https://doi.org/10.1007/s00216-017-0268-z

[73] R. Junjuri, M.K. Gundawar, 2023. Plastic Waste Identification Using Laser-Induced Breakdown Spectroscopy. Laser Induced Breakdown Spectroscopy (LIBS) Concepts, Instrumentation, Data Analysis and Applications. 2, 615-622. https://doi.org/10.1002/9781119758396.ch29

[74] S. Barbier, S. Perrier, P. Freyermuth, D. Perrin, B. Gallard, N. Gilon, 2013. Plastic identification based on molecular and elemental information from laser induced breakdown

spectra: a comparison of plasma conditions in view of efficient sorting. Spectrochimica Acta Part B: Atomic Spectroscopy. 88, 167-173. https://doi.org/10.1016/j.sab.2013.06.007

[75] Y. Li, M.A. Nahil, P.T. Williams, 2023. Pyrolysis-catalytic steam reforming of waste plastics for enhanced hydrogen/syngas yield using sacrificial tire pyrolysis char catalyst. Chemical Engineering Journal. 467, 143427. https://doi.org/10.1016/j.cej.2023.143427

[76] S.H. Cho, Y. Kim, S. Lee, K.Y.A. Lin, W.H. Chen, S. Jung, D. Lee, D.H. Moon, Y.J. Jeon, E.E. Kwon, 2023. Virtuous utilization of carbon dioxide in pyrolysis of polylactic acid. Chemical Engineering Journal. 466, 143307. https://doi.org/10.1016/j.cej.2023.143307

[77] R. Zou, C. Wang, M. Qian, R. Lei, Y. Zhao, Q. Zhang, E. Huo, X. Kong, X. Lin, L. Wang, X. Zhang, 2023. Catalytic fast co-pyrolysis of Douglas Fir and low-density polyethylene with nanocellulose-derived carbon catalyst for enhancing selectivity of hydrogen in syngas and mono-aromatic hydrocarbon in bio-oil products. Chemical Engineering Journal. 474, 145640. https://doi.org/10.1016/j.cej.2023.145640

[78] Y. Zeng, Z. Liu, J. Yu, E. Hu, X. Jia, Y. Tian, C. Wang, 2024. Pyrolysis kinetics and characteristics of waste tyres: Products distribution and optimization via TG-FTIR-MS and rapid infrared heating techniques. Chemical Engineering Journal. 482, 149106. https://doi.org/10.1016/j.cej.2024.149106

[79] H. Yokota, T. Kawakami, S. Nagayama, K. Okazaki, E. Makuuchi, Y. Abe, M. Otaka, 2023. A New Laser Induced Breakdown Spectroscopy (LIBS) Spectral Data Analysis Method Using No Database Reference or Peak Wavelength Search. Journal of Japan Society for Fuzzy Theory and Intelligent Informatics. 35(1), 561-566. https://doi.org/10.3156/jsoft.35.1_561

[80] A.R. Striganov, N.S. Sventitskii, 2013. Tables of spectral lines of neutral and ionized atoms. Springer Science & Business Media. https://doi.org/10.1007/978-1-4757-6610-3

[81] J. Orszagh, B. Stachova, J. Blasko, S. Matejcik, D. Bodewits, S. Bromley, 2022. Reference emission spectral data for astronomical observations. In European Planetary Science Congress. EPSC2022-950. https://doi.org/10.5194/epsc2022-950

[82] A.P. Michel, A.E. Morrison, V.L. Preston, C.T. Marx, B.C. Colson, H.K. White, 2020. Rapid identification of marine plastic debris via spectroscopic techniques and machine learning classifiers. Environmental Science & Technology. 54(17), 10630-10637. https://doi.org/10.1021/acs.est.0c02099

[83] D. Dubey, R. Kumar, A. Dwivedi, A.K. Rai, 2022. Study of electronic bands of diatomic molecules for the evaluation of toxicity of green crackers using LIBS coupled with chemometric method. Electronic Materials. 4(1), 1-14. https://doi.org/10.3390/electronicmat4010001

[84] G. Gautam, C.G. Parigger, D.M. Surmick, A.M.E. Sherbini, 2016. Laser plasma diagnostics and self-absorption measurements of the Hβ Balmer series line. Journal of Quantitative Spectroscopy and Radiative Transfer. 170, 189-193. https://doi.org/10.1016/j.jqsrt.2015.11.011

[85] Y. Chen, X. Man, B. Liu, Z. Lin, 2023. Nitrogen fluorescence emission pumped by femtosecond optical vortex beams. Frontiers in Physics. 11, 1124026. https://doi.org/10.3389/fphy.2023.1124026

[86] T. Dequaire, P.Y. Meslin, P. Beck, M. Jaber, A. Cousin, W. Rapin, J. Lasue, O. Gasnault, S. Maurice, A. Buch, C. Szopa, 2017. Analysis of carbon and nitrogen signatures with laser-induced breakdown spectroscopy; the quest for organics under Mars-like conditions. Spectrochimica Acta Part B: Atomic Spectroscopy. 131, 8-17. https://doi.org/10.1016/j.sab.2017.02.015

[87] Y.E.E.D. Gamal, K.A. Elsayed, O.A. Nassef, 2021. Study of Electron Dynamics Controlling the Threshold Intensity Dependence on the Gas Pressure in FIR Laser-Induced Breakdown of Molecular Oxygen: Effect of Loss Processes. Arabian Journal for Science and Engineering. 46, 5875-5884. https://doi.org/10.1007/s13369-020-05077-2

[88] V. Wakelam, I.W.M. Smith, E. Herbst, J. Troe, W. Geppert, H. Linnartz, K. Öberg, E. Roueff, M. Agúndez, P.E. Pernot, H.M. Cuppen, 2010. Reaction networks for interstellar chemical modelling: improvements and challenges. Space Science Reviews. https://doi.org/10.1007/s11214-010-9712-5

[89] S. Schröder, K. Rammelkamp, D.S. Vogt, O. Gasnault, H.W. Hübers, 2019. Contribution of a martian atmosphere to laser-induced breakdown spectroscopy (LIBS) data and testing its emission characteristics for normalization applications. Icarus. 325, 1-15. https://doi.org/10.1016/j.icarus.2019.02.017

[90] N.H. Thomas, B.L. Ehlmann, D.E. Anderson, S.M. Clegg, O. Forni, S. Schröder, W. Rapin, P.Y. Meslin, J. Lasue, D.M. Delapp, M.D. Dyar, 2018. Characterization of hydrogen in basaltic materials with laser-induced breakdown spectroscopy (LIBS) for application to MSL ChemCam data. Journal of Geophysical Research: Planets. 123(8), 1996-2021. https://doi.org/10.1029/2017je005467

[91] K. Liu, D. Tian, C. Li, Y. Li, G. Yang, Y. Ding, 2019. A review of laser-induced breakdown spectroscopy for plastic analysis. TrAC Trends in Analytical Chemistry. 110, 327-334. https://doi.org/10.1016/j.trac.2018.11.025

[92] S.N. Abdulmadjid, B.S. Hartadi, R. Mitaphonna, M. Iqhrammullah, 2023. Discrimination of Plastic Waste using Laser-induced Breakdown Spectroscopy-principal Component Analysis: Highlighting Molecular LIBS. International Journal of Engineering. 36(1), 98-107. https://doi.org/10.5829/ije.2023.36.01a.12

[93] J.W. Daiber, J.G. Winans, 1968. Radiation from laser-heated plasmas in nitrogen and argon. JOSA. 58(1), 76-80. https://doi.org/10.1364/josa.58.000076

[94] Z. Gajarska, L. Brunnbauer, H. Lohninger, A. Limbeck, 2021. Identification of 20 polymer types by means of laser-induced breakdown spectroscopy (LIBS) and chemometrics. Analytical and Bioanalytical Chemistry. 413(26), 6581-6594. https://doi.org/10.1007/s00216-021-03622-y

[95] J.L. Gottfried, T.M. Klapötke, T.G. Witkowski, 2017. Estimated Detonation Velocities for TKX-50, MAD-X1, BDNAPM, BTNPM, TKX-55, and DAAF using the Laser–induced Air Shock from Energetic Materials Technique. Propellants, Explosives, Pyrotechnics. 42(4), 353-359. https://doi.org/10.1002/prep.201600257

[96] J. Moros, J. Laserna, 2019. Laser-induced breakdown spectroscopy (LIBS) of organic compounds: A review. Applied Spectroscopy. 73(9), 963-1011. https://doi.org/10.1177/0003702819853252

[97] K. Sovová, K. Dryahina, P. Španěl, M. Kyncl, S. Civiš, 2010. A study of the composition of the products of laser-induced breakdown of hexogen, octogen, pentrite and trinitrotoluene using selected ion flow tube mass spectrometry and UV-Vis spectrometry. Analyst. 135(5), 1106-1114. https://doi.org/10.1039/b926425f

[98] R.W.B. Pearse, A.G. Gaydon, R.W.B. Pearse, A.G. Gaydon, 1976. The identification of molecular spectra. London: Chapman and Hall. https://doi.org/10.1007/978-94-009-5758-9

[99] R.S. Ram, P.F. Bernath, 2012. Fourier transform emission spectroscopy of the A2Π–X2Σ+(red) system of 13C14N (II). Journal of Molecular Spectroscopy. 274, 22-27. https://doi.org/10.1016/j.jms.2012.03.008

[100] A. Kushwaha, R.K. Thareja, 2008. Dynamics of laser-ablated carbon plasma: formation of C2 and CN. Applied Optics. 47(31), G65-G71. https://doi.org/10.1364/ao.47.000g65

[101] D. Carinhana Jr, L.G. Barreta, C.J. Rocha, A.M.D. Santos, C.A. Bertran, 2008. Determination of liquefied petroleum flame temperatures using emission spectroscopy. Journal of the Brazilian Chemical Society. 19, 1326-1335. https://doi.org/10.1590/s0103-50532008000700015

[102] Q.S. Yang, J.H. Song, N.Y. Zhu, 2012. Determination of temperatures using CH radical emission spectroscopy. Chinese Physics Letters. 29(10), 104707. https://doi.org/10.1088/0256-307x/29/10/104707

[103] M.N. Siddiqui, M.A. Gondal, H.H. Redhwi, 2008. Identification of different type of polymers in plastics waste. Journal of Environmental Science and Health, Part A. 43(11), 1303-1310. https://doi.org/10.1080/10934520802177946

[104] M. Zachwieja, W. Szajna, R. Hakalla, 2012. The A2Δ–X2Π band system of the CD radical. Journal of Molecular Spectroscopy. 275, 53-60. https://doi.org/10.1016/j.jms.2012.05.006

[105] G. de Izarra, J.M. Cormier, 2013. New methods to determine temperatures from UV OH spectrum. Journal of Physics D: Applied Physics. 46(10), 105503. https://doi.org/10.1088/0022-3727/46/10/105503

[106] P. Jenniskens, C.O. Laux, 2004. Search for the OH (X 2Π) Meinel Band Emission in Meteors as a Tracer of Mineral Water in Comets: Detection of N2+ (AX). Astrobiology. 4(1), 109-121. https://doi.org/10.1089/153110704773600276

[107] Q. Zeng, J.B. Sirven, J.C.P. Gabriel, C.Y. Tay, J.M. Lee, 2021. Laser induced breakdown spectroscopy for plastic analysis. TrAC Trends in Analytical Chemistry. 140, 116280. https://doi.org/10.1016/j.trac.2021.116280

[108] M. Sabsabi, 2022. LIBS Fundamentals. Chemometrics and Numerical Methods in LIBS. 5-18. https://doi.org/10.1002/9781119759614.ch1

[109] F. Xu, S. Ma, C. Zhao, D. Dong, 2022. Application of molecular emissions in laser-induced breakdown spectroscopy: a review. Frontiers in Physics. 10, 821528. https://doi.org/10.3389/fphy.2022.821528

[110] H.M. Ruiz, F. Guzmán, M. Favre, H. Bhuyan, H. Chuaqui, E.S. Wyndham, 2012. Time- and space-resolved spectroscopic characterization of a laser carbon plasma plume in an argon background. Plasma Sources Science and Technology. 21(3), 034014. https://doi.org/10.1088/0963-0252/21/3/034014

[111] L. Nemes, A.M. Keszler, C.G. Parigger, J.O. Hornkohl, H.A. Michelsen, V. Stakhursky, 2007. Spontaneous emission from the C3 radical in carbon plasma. Applied Optics. 46(19), 4032-4040. https://doi.org/10.1364/ao.46.004032

[112] C.G. Parigger, J.O. Hornkohl, L. Nemes, 2011. Time-Resolved Spectroscopy Diagnostic of Laser-Induced Optical Breakdown. International Journal of Spectroscopy (Online). 2011. https://doi.org/10.1155/2010/593820

[113] N.U. Rehman, A. Masood, Z. Anjum, I. Ahmad, M.A. Khan, M. Zakaullah, 2015. Optical emission spectroscopy of He–N2 mixture plasma. Radiation Effects and Defects in Solids. 170(7-8), 668-678. https://doi.org/10.1080/10420150.2015.1083993

[114] M. Park, Y. Gu, X. Mao, C.P. Grigoropoulos, V. Zorba, 2023. Mechanisms of ultrafast GHz burst fs laser ablation. Science Advances. 9(12), eadf6397. https://doi.org/10.1126/sciadv.adf6397

[115] J. Serrano, J. Moros, J.J. Laserna, 2016. Molecular signatures in femtosecond laser-induced organic plasmas: comparison with nanosecond laser ablation. Physical Chemistry Chemical Physics. 18(4), 2398-2408. https://doi.org/10.1039/c5cp06456b

[116] E. Thiele, M.F. Goodman, J. Stone, 1980. Can lasers be used to break chemical bonds selectively?. Optical Engineering. 19(1), 10-20. https://doi.org/10.1117/12.7972464

[117] M. Soleimani, P. Peng, W. Duley, Y.N. Zhou, 2023. Selective breaking and re-joining of CuO nanowires by nanosecond laser irradiation. Journal of Applied Physics. 133(7). https://doi.org/10.1063/5.0136406

[118] A.K. Misra, T.E. Acosta-Maeda, J.N. Porter, G. Berlanga, D. Muchow, S.K. Sharma, B. Chee, 2019. A two components approach for long range remote Raman and laser-induced breakdown (LIBS) spectroscopy using low laser pulse energy. Applied Spectroscopy. 73(3), 320-328. https://doi.org/10.1177/0003702818812144

[119] P. Zhou, Y. Zhu, S. Li, L.G. Zhu, 2018. Reutilization of nanosecond pulse laser energy and its performance in single particle triggered LIBS. RSC Advances. 8(73), 41915-41919. https://doi.org/10.1039/c8ra06985a

[120] L. Wu, Y. Guan, C. Li, L. Shi, S. Yang, B.R. Reddy, G. Ye, Q. Zhang, R.K. Liew, J. Zhou, R. Vinu, 2023. Free-radical behaviors of co-pyrolysis of low-rank coal and different solid hydrogen-rich donors: A critical review. Chemical Engineering Journal. 145900. https://doi.org/10.1016/j.cej.2023.145900

[121] H. Kim, J. Lee, Y. Kim, J.M. Ha, Y.K. Park, D.G. Vlachos, Y.W. Suh, J. Jae, 2024. Continuous flow upgrading of lignin pyrolysis oils to drop-in bio-hydrocarbon fuels over noble metal catalysts. Chemical Engineering Journal. 481, 148328. https://doi.org/10.1016/j.cej.2023.148328

[122] Q. Yang, Q. Wu, N. Zhou, L. Ke, L. Fan, Y. Zeng, C. Xu, Y. Liu, R. Ruan, Y. Wang, 2023. Continuous catalytic pyrolysis of waste oil to aromatics: Exploring the structure-performance relations of ZSM-5 based on different scale-up forms. Chemical Engineering Journal. 475, 146259. https://doi.org/10.1016/j.cej.2023.146259

[123] X. Lin, X. Chen, P. Fu, B. Tang, D. Bi, 2023. Highly efficient production of monocyclic aromatics from catalytic co-pyrolysis of biomass and plastic with nitrogen-doped activated carbon catalyst. Chemical Engineering Journal. 474, 145783. https://doi.org/10.1016/j.cej.2023.145783

[124] Y. Zeng, Y. Wang, Q. Wu, Q. Zhang, X. Cui, L. Ke, X. Tian, J. Xu, R. Zou, K. Bob, Y. Liu, 2023. Microwave-assisted catalytic co-pyrolysis of waste edible oil and low-density polyethylene: Synergistic enhancement of co-melt feeding. Chemical Engineering Journal. 459, 141567. https://doi.org/10.1016/j.cej.2023.141567

[125] M. Mokashi, A.B. Shirsath, P. Lott, H. Müller, S. Tischer, L. Maier, O. Deutschmann, 2024. Understanding of gas-phase methane pyrolysis towards hydrogen and solid carbon with detailed kinetic simulations and experiments. Chemical Engineering Journal. 479, 147556. https://doi.org/10.1016/j.cej.2023.147556

[126] X. Yue, J. Lin, T. Suopajärvi, O. Mankinen, A. Mikkelson, R. Liu, H. Huttunen, L. Chen, C. Xu, V.V. Telkki, S. Sun, 2023. Conversion of highly polymerized lignin into monophenolic products via pyrolysis: A comparative study of acidic and alkaline depolymerization pretreatments using deep eutectic solvents. Chemical Engineering Journal. 478, 147368. https://doi.org/10.1016/j.cej.2023.147368

[127] L. Zhang, Q. Wu, L. Fan, R. Liao, J. Zhang, R. Zou, K. Cobb, R. Ruan, Y. Wang, 2024. Monocyclic aromatic hydrocarbons production from NaOH pretreatment metallized food plastic packaging waste through microwave pyrolysis coupled with ex-situ catalytic reforming. Chemical Engineering Journal. 149777. https://doi.org/10.1016/j.cej.2024.149777

[128] G. Zhu, M. Zhu, E. Wang, C. Gong, Y. Wang, W. Guo, G. Xie, W. Chen, C. He, L. Xu, H. Li, 2024. Natural biochar catalyst: Realizing the co-valorization of waste cooking oil into high-

quality biofuel and carbon nanotube precursor via catalytic pyrolysis process. Chemical Engineering Journal. 486, 150195. https://doi.org/10.1016/j.cej.2024.150195

[129] Z. Zong, N. Koers, G. Cai, D.C. Upham, 2024. CO2-to-methanol: Economic and environmental comparison of emerging and established technologies with dry reforming and methane pyrolysis. Chemical Engineering Journal. 487, 150274. https://doi.org/10.1016/j.cej.2024.150274

[130] L. Wu, J. Liu, L. Chen, X. Wang, Q. Zhou, F. Yu, J. Liang, 2024. Hierarchical beta zeolites assisted aromatics production from lignin via catalytic fast pyrolysis. Chemical Engineering Journal. 149618. https://doi.org/10.1016/j.cej.2024.149618

[131] B. Cao, N. Jiang, M. Jiao, R. Ren, T. Zhang, 2024. Enhancing hydrogen-rich fuel gas production from dewatered sludge pyrolysis: The effect of hybrid conditioning with peroxyacetic acid, polyaluminium chloride, and KOH-modified activated carbon. Chemical Engineering Journal. 479, 147733. https://doi.org/10.1016/j.cej.2023.147733

[132] D. Sangaré, M. Moscosa-Santillan, S. Bostyn, V. Belandria, A. De la Cruz Martínez, L. Van De Steene, 2024. Multi-step kinetic mechanism coupled with CFD modeling of slow pyrolysis of biomass at different heating rates. Chemical Engineering Journal. 479, 147791. https://doi.org/10.1016/j.cej.2023.147791

[133] S. Orozco, L. Santamaria, M. Artetxe, J. Alvarez, J. Bilbao, M. Olazar, G. Lopez, 2023. Influence of oxidative conditions on the deactivation of an equilibrium FCC catalyst in the fast pyrolysis of HDPE in a conical spouted bed reactor. Chemical Engineering Journal. 472, 144947. https://doi.org/10.1016/j.cej.2023.144947

[134] Y.W. Cheah, R. Intakul, M.A. Salam, J. Sebastian, P.H. Ho, P. Arora, O. Öhrman, D. Creaser, L. Olsson, 2023. Slurry co-hydroprocessing of Kraft lignin and pyrolysis oil over unsupported NiMoS catalyst: A strategy for char suppression. Chemical Engineering Journal. 475, 146056. https://doi.org/10.1016/j.cej.2023.146056

[135] N. Raja, G.M. Monsalve-Bravo, Y.V. Kaneti, J. Mensah, K. Wilson, A.F. Lee, M. Konarova, 2023. Thermogravimetric kinetic analysis of catalytic and non-catalytic pyrolysis of simulated municipal solid waste. Chemical Engineering Journal. 470, 144046. https://doi.org/10.1016/j.cej.2023.144046

[136] J. Xiao, G. Fang, X. Jin, B. Wang, S. Meng, 2023. A comprehensive study of pyrolysis characteristics of silicone-modified phenolic aerogel matrix Nanocomposites: Kinetic Analysis, ReaxFF MD Simulations, and ANN prediction. Chemical Engineering Journal. 472, 145049. https://doi.org/10.1016/j.cej.2023.145049

[137] C. Huang, B.A. Mohamed, L.Y. Li, 2023. Comparative life-cycle energy and environmental analysis of sewage sludge and biomass co-pyrolysis for biofuel and biochar production. Chemical Engineering Journal. 457, 141284. https://doi.org/10.1016/j.cej.2023.141284

[138] T. Delgado, J.M. Vadillo, J.J. Laserna, 2014. Pressure effects in laser-induced plasmas of trinitrotoluene and pyrene by laser-induced breakdown spectroscopy (LIBS). Applied Spectroscopy. 68(1), 33-38. https://doi.org/10.1366/13-07164

[139] W. Feng, M. Zheng, J. Bai, X. Zhang, C. Wu, Z. Guo, L. Kong, Z. Bai, W. Li, 2023. Dynamic structure transformation of char precursors during co-pyrolysis of coal and HDPE by using ReaxFF MD simulation and experiments. Chemical Engineering Journal. 472, 145100. https://doi.org/10.1016/j.cej.2023.145100

[140] Xuan, Weiwei, Jian Gao, Zhen Ma, Chunyan Cao, Shiying Yan, and Qi Wang. "Synergistic mechanism and radicals interaction of the co-pyrolysis of lignite and PE based on ReaxFF-MD and DFT." *Energy* 289 (2024): 129978. https://doi.org/10.1016/j.energy.2023.129978

[141] B.A. Perez, J.J. Krishna, H.E. Toraman, 2023. Insights into co-pyrolysis of polyethylene terephthalate and polyamide 6 mixture through experiments, kinetic modeling and machine learning. Chemical Engineering Journal. 468, 143637. https://doi.org/10.1016/j.cej.2023.143637

[142] A. Asghar, C.G. Liu, I. Ali, A.Z. Khan, H. Zhu, N. Wang, M. Nawaz, T.A. Tabish, M.A. Mehmood, R.T. Rasool, 2023. Bioenergy potential of Saccharum bengalense through pyrolysis, reaction kinetics, TG-FTIR-GCMS analysis of pyrolysis products, and validation of the pyrolysis data through machine learning. Chemical Engineering Journal. 465, 142930. https://doi.org/10.1016/j.cej.2023.142930

[143] H.K. Eidesen, H. Khawaja, S. Jackson, 2018. Simulation of the HDPE pyrolysis process. https://doi.org/10.21152/1750-9548.12.1.79

[144] R.A.U. Nabi, H. Hussain, M.Y. Naz, S. Shukrullah, H.A. Khawaja, M. Irfan, S. Rahman, A.A.J. Ghanim, 2023. Sensitivity analysis of thermal degradation of plastic waste using statistically assumed exponential factors and activation energies. ACS Omega. 8(15), 14122-14130. https://doi.org/10.1021/acsomega.3c00801

[145] R.A.U. Nabi, M.Y. Naz, S. Shukrullah, M. Ghamkhar, N.U. Rehman, M. Irfan, A.O. Alqarni, S. Legutko, I. Kruszelnicka, D. Ginter-Kramarczyk, M. Ochowiak, 2022. Analysis of statistically predicted rate constants for pyrolysis of high-density plastic using R software. Materials. 15(17), 5910. https://doi.org/10.3390/ma15175910

[146] M. Irfan, R.A.U. Nabi, H. Hussain, M.Y. Naz, S. Shukrullah, H.A. Khawaja, S. Rahman, A.A. Ghanim, I. Kruszelnicka, D. Ginter-Kramarczyk, S. Legutko, 2022. Response Surface Methodology Analysis of Pyrolysis Reaction Rate Constants for Predicting Efficient Conversion of Bulk Plastic Waste into Oil and Gaseous Fuels. Energies. 15(24), 9594. https://doi.org/10.3390/en15249594

[147] W.H. Chen, P.P. Biswas, E.E. Kwon, Y.K. Park, S. Rajendran, L. Gnanasekaran, J.S. Chang, 2023. Optimization of the process parameters of catalytic plastic pyrolysis for oil production using design of experiment approaches: A review. Chemical Engineering Journal. 144695. https://doi.org/10.1016/j.cej.2023.144695

[148] F. Carretta, S. Pelucchi, F. Galli, P. Mocellin, 2024. Methane pyrolysis for hydrogen production: Modeling of soot deposition by computational fluid dynamics and experimental validation. Chemical Engineering Journal. 149844. https://doi.org/10.1016/j.cej.2024.149844

[149] M.P. Ruiz, D.M. Zairin, S.R. Kersten, 2023. On the intrinsic reaction rate of polyethylene pyrolysis and its interplay with mass transfer. Chemical Engineering Journal. 469, 143886. https://doi.org/10.1016/j.cej.2023.143886

[150] Q. Al-Naddaf, A.A. Rownaghi, F. Rezaei, 2020. Multicomponent adsorptive separation of CO2, CO, CH4, N2, and H2 over core-shell zeolite-5A@ MOF-74 composite adsorbents. Chemical Engineering Journal. 384, 123251. https://doi.org/10.1016/j.cej.2019.123251

[151] M.X. Xu, J.Y. Di, Y.C. Wu, X.X. Meng, H. Jiang, J.H. Li, Q. Lu, 2023. Insights into the pyrolysis mechanisms of epoxy resin polymers based on the combination of experiments and ReaxFF-MD simulation. Chemical Engineering Journal. 473, 145404. https://doi.org/10.1016/j.cej.2023.145404

[152] R.A.U. Nabi, M.Y. Naz, S. Shukrullah, M. Ghamkhar, N.U. Rehman, M. Irfan, A.O. Alqarni, S. Legutko, I. Kruszelnicka, D. Ginter-Kramarczyk, M. Ochowiak, 2022. Analysis of statistically predicted rate constants for pyrolysis of high-density plastic using R software. Materials. 15(17), 5910. https://doi.org/10.3390/ma15175910

[153] A.O. Alqarni, R.A.U. Nabi, F. Althobiani, M.Y. Naz, S. Shukrullah, H.A. Khawaja, M.A. Bou-Rabee, M.E. Gommosani, H. Abdushkour, M. Irfan, M.H. Mahnashi, 2022. Statistical optimization of pyrolysis process for thermal destruction of plastic waste based on temperature-dependent activation energies and pre-exponential factors. Processes. 10(8), 1559. https://doi.org/10.3390/pr10081559

[154] M. Irfan, R.A.U. Nabi, H. Hussain, M.Y. Naz, S. Shukrullah, H.A. Khawaja, S. Rahman, M.U. Farid, 2023. Statistical prediction and sensitivity analysis of kinetic rate constants for efficient thermal valorization of plastic waste into combustible oil and gases. Heliyon. 9(5). https://doi.org/10.1016/j.heliyon.2023.e16049

[155] M. Irfan, R.A.U. Nabi, H. Hussain, M.Y. Naz, S. Shukrullah, H.A. Khawaja, S. Rahman, F. Althobiani, 2023. Numerical sensitivity analysis of temperature-dependent reaction rate constants for optimized thermal conversion of high-density plastic waste into combustible fuels. The Canadian Journal of Chemical Engineering. 101(10), 5611-5620. https://doi.org/10.1002/cjce.24883

Graphical Abstract

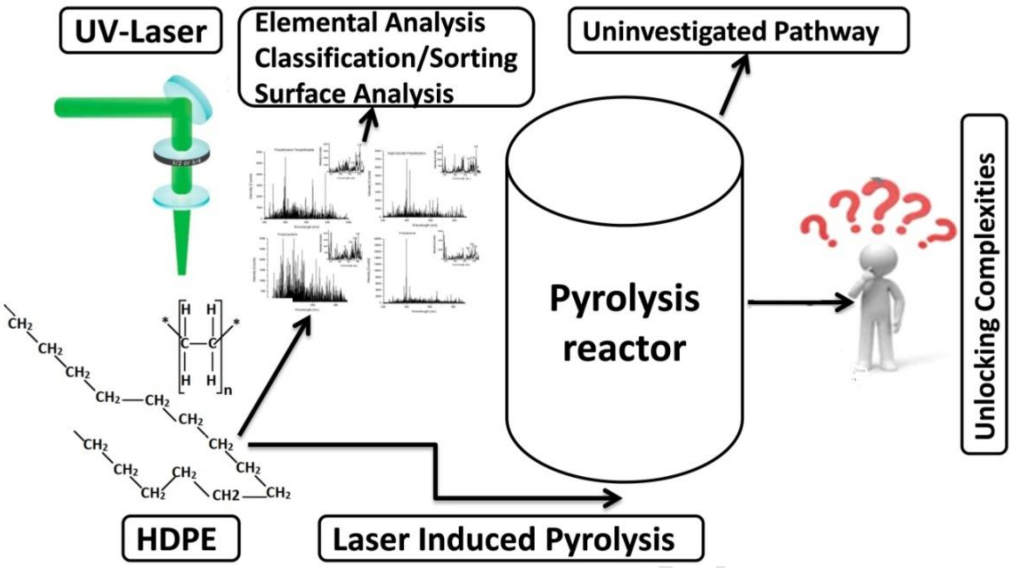

Highlights

Primary Objective:

- Evaluating LIBS for plastic polymers, emphasizing HDPE

Secondary Objectives:

- To investigate LIBS for HDPE bond-breaking
- To analyze undocumented LIBS Spectra of Key Products
- Analysis of C-C and C-H bonds durability in HDPE
- To investigate the potential of Laser-Induced HDPE Pyrolysis